THESIS FOR THE DEGREE OF DOCTOR OF PHILOSOPHY

ALTERNATIVE POLYETHYLENE CROSSLINKING CONCEPTS FOR POWER CABLE INSULATION

MASSIMILIANO MAURI

Department of Chemistry and Chemical Engineering

CHALMERS UNIVERSITY OF TECHNOLOGY

Gothenburg, Sweden 2019

ALTERNATIVE POLYETHYLENE CROSSLINKING CONCEPTS FOR POWER CABLE INSULATION

MASSIMILIANO MAURI

ISBN 978-91-7597-841-3

Doktorsavhandlingar vid Chalmers tekniska högskola
Ny serie nr 4522
ISSN 0346-718X

Department of Chemistry and Chemical Engineering
Chalmers University of Technology
SE-412 96 Gothenburg
Sweden
Telephone + 46 (0)31-772 1000

Cover: Optical micrographs of thin films of p(E-*stat*-GMA_8) (blue), p(E-*stat*-AA_7) (yellow) and p(E-*stat*-GMA_8):p(E-*stat*-AA_7) blend (pink) prepared by drop-casting from 10 g L^{-1} hot p-xylene solutions.

Chalmers Reproservice
Gothenburg, Sweden 2019

ALTERNATIVE POLYETHYLENE CROSSLINKING CONCEPTS FOR POWER CABLE INSULATION

MASSIMILIANO MAURI

Department of Chemistry and Chemical Engineering
Chalmers University of Technology – Gothenburg, Sweden

Abstract

We currently witness an accelerating shift from fossil energy sources to renewables driven by the urgent need to reduce carbon emissions. Wind, solar and hydro power is most abundant in places far away from the end user, which necessitates the efficient transport of electricity over long distances. Alternative grid designs are needed that complement high-voltage alternating current (HVAC) with high-voltage direct current (HVDC) cables. The most advanced power cable technology uses crosslinked polyethylene (XLPE) insulation, which is produced by peroxide crosslinking of low-density polyethylene (LDPE). However, peroxide crosslinking gives rise to by-products that compromise the cleanliness of LDPE and raise the electrical conductivity of the insulation material. Therefore, a by-product free curing process, which maintains the processing advantages and high electrical resistivity of LDPE, would considerably ease cable manufacturing and is therefore in high demand.

This thesis introduces alternative concepts for the crosslinking of polyethylene that fulfil these requirements. In particular, the suitability of click-chemistry epoxy ring opening reactions for curing of an ethylene-glycidyl methacrylate copolymer has been explored. Three main concepts for by-product free cable insulation have been studied: (i) crosslinking of LDPE copolymers with low molecular-weight multifunctional curing agents, (ii) Lewis acid assisted crosslinking of LDPE copolymer formulations, and (iii) reactive blending of LDPE copolymers. This thesis summarizes extensive characterization of the curing process and the resulting thermo-mechanical properties of the materials, as well as preliminary conductivity studies. It can be anticipated that the concepts introduced in this thesis may lead to a by-product free and sustainable alternative to peroxide-based crosslinking of polyethylenes.

Keywords: *High-voltage insulation, polyethylene, crosslinking, epoxy, click-chemistry, polymer blends*

Contents

List of Publications

The thesis is based on the following papers, referred to by Roman numerals in the text.

Paper I. **Crosslinking of an ethylene-glycidyl methacrylate copolymer with amine click chemistry**

Massimiliano Mauri, Nina Tran, Oscar Prieto, Thomas Hjertberg, Christian Müller

Polymer **2017**, *111*, 27-35.

Paper II. **Orange is the new white: Rapid curing of an ethylene-glycidyl methacrylate copolymer with a Ti-bisphenolate type catalyst**

Massimiliano Mauri, Leo Svenningsson, Thomas Hjertberg, Lars Nordstierna, Oscar Prieto, Christian Müller

Polymer Chemistry, **2018**, *9*, 1710-1718.

Paper III. **Byproduct-free curing of a highly insulating polyethylene copolymer blend: An alternative to peroxide crosslinking**

Massimiliano Mauri, Anna Peterson, Ayça Senol, Khalid Elamin, Antonis Gitsas, Thomas Hjertberg, Aleksandar Matic, Thomas Gkourmpis, Oscar Prieto, Christian Müller

Journal of Materials Chemistry C, **2018**, *6*, 11292-11302.

Paper IV. **Click chemistry crosslinking of a low-conductivity polyethylene copolymer ternary blend for power cable insulation**

Massimiliano Mauri, Anna I. Hofmann, Diana Gómez-Heincke, Per-Ola Hagstrand, Thomas Gkourmpis, Oscar Prieto, Christian Müller

Manuscript.

Contribution Report

Paper I. Main author, responsible for the design of experiments, sample preparation, data collection and data analysis. O. Prieto and C. Müller assisted the author with invaluable scientific inputs. The first draft of the manuscript was written together with C. Müller and afterwards revised by all coauthors.

Paper II. Main author, responsible for the design of experiments, sample preparation, data collection and data analysis. O. Prieto and C. Müller assisted the author with invaluable scientific inputs. Solid state NMR was performed by L. Svenningsson. The first draft of the manuscript was written together with C. Müller and afterwards revised by all coauthors.

Paper III. Main author, together with A. Peterson responsible for the design of experiments, sample preparation, data collection and data analysis. O. Prieto and C. Müller assisted the author with invaluable scientific and conceptual inputs. FTIR and DSC analysis were performed by A. Peterson. BDS experiments and data analysis were performed by T. Gkourmpis and A. Gitsas. The first draft of the manuscript was written together with A. Peterson and C. Müller, and afterwards revised by all coauthors.

Paper IV. Main author, responsible for the design of experiments, sample preparation and data analysis. O. Prieto, P.-O. Hagstrand and C. Müller assisted the author with invaluable conceptual inputs. Rheology measurements were performed together with D. Gómez-Heincke. AFM measurements were performed by A. Hofmann. BDS experiments and data analysis were performed by T. Gkourmpis. The first draft of the manuscript was written together with C. Müller.

Publications not included in the thesis

Paper 1. **Copolymerization of ethylene with α-olefins and cyclic olefins catalyzed by a Ti(IV) diisopropoxy complex bearing a tridentate [O−,S,O−]-type bis(phenolato) ligand**

Giuseppe Leone, Massimiliano Mauri, Simona Losio, Fabio Bertini, Giovanni Ricci, Lido Porri

Polymer Chemistry, **2014**, *5*, 3412-3423.

Paper 2. **Ni(II) α-Diimine-Catalyzed α-Olefins Polymerization: Thermoplastic Elastomers of Block Copolymers**

Giuseppe Leone, Massimiliano Mauri, Fabio Bertini, Maurizio Canetti, Daniele Piovani, Giovanni Ricci

Macromolecules, **2015**, *48 (5)*, 1304-1312.

Paper 3. **Polyolefin thermoplastic elastomers from 1-octene chain-walking polymerization**

Giuseppe Leone, Massimiliano Mauri, Ivana Pierro, Giovanni Ricci, Maurizio Canetti, Fabio Bertini

Polymer, **2016**, *100*, 37-44.

Paper 4. **Perfectly Alternating Ethylene/2-Butene Copolymers by Hydrogenation of Highly Stereoregular 1,4-Poly(1,3-diene)s: Synthesis and Characterization**

Giovanni Ricci, Giuseppe Leone, Antonella Caterina Boccia, Ivana Pierro, Giorgia Zanchin, Massimiliano Mauri, Miriam Scoti, Anna Malafronte, Finizia Auriemma, Claudio De Rosa

Macromolecules, **2017**, *50 (3)*, 754-761.

“La verità non cambia perché è, o non è, creduta dalla maggioranza delle persone.”

“Truth does not change because it is, or is not, believed by the majority of the people.”

Giordano Bruno (Nola, 1548 – Roma, Campo de' Fiori, 17 febbraio 1600)

CHAPTER 1

1.1 Historical milestones in the development of High Voltage cable technology

The early years of the electricity supply industry, dating to the end of the 19th century, were characterized by a fierce competition between the proponents of direct current (DC) and alternating current (AC) over which type of technology ought to be used for the transportation of electricity. The use of DC was promoted by Thomas Edison as a safe means of electricity transport, in open competition with the use of AC as advocated by several European companies and by Westinghouse Electric, which had acquired many of the patents by Nikola Tesla. This fierce competition eventually ended with a victory for AC, mostly thanks to the possibility to easily increase and decrease the voltage through the use of transformers. AC has maintained its dominance for almost all domestic and industrial supplies of electricity since then, but with the growth of the electricity supply system in size the limitations of AC technology have started to emerge. For instance, due to AC system related reactive and resistive losses, it is challenging to transfer electricity over very long distances. The maximum length of an AC cable is limited by its high capacitance, which causes a phase difference θ between voltage V and current I. The useful active power P can be expressed as:[1, 2]

$$P = VI \mid cos\theta \mid \quad (1)$$

The remaining power is transformed into reactive power Q:

$$Q = VI \mid sin\theta \mid \quad (2)$$

The reactive power increases both with cable length and voltage.[1, 3] For example, the maximum transmission length for XLPE insulated AC cable systems with a 1000 mm^2 Cu conductor, which is able to transfer at least 80 % of the current, is ~ 100 km at 110 kV. This length is further reduced at higher voltages, reaching only ~ 50 km if the cables are operated at 380 kV.[1, 4] For long distance transmission high voltage direct current (HVDC) is more efficient as compared to AC systems.[3]

The advantages of HVDC for long distance transmission were known, but its use was held back by the lack of a suitable technology that could convert DC to AC and vice versa. The invention of the mercury arc rectifier in the late 1920s was a major breakthrough in the field of HVDC systems, but this pioneering development did not see commercial use until 1954, when the first HVDC cable was installed in Sweden. The system, named Gotland 1 (or Gotland Link), consisted of a 98 km long HVDC undersea cable that operated at 80 kV and was able to transfer up to 20 MW,[5] connecting the Swedish mainland from the city of Västervik to Ygne on the island of Gotland. Mercury arc valves were used as a static inverter, marking the beginning of the mercury arc era during which 11 HVDC cable systems were built all over the world, spanning from New Zealand to Japan, North America and Europe.

Almost concurrently, a new technology that would later replace the mercury arc valves was introduced: the silicon semiconductor thyristor. A thyristor is a solid-state semiconductor device with four layers of alternating P-type and N-type materials that can convert between DC and AC, switching power on the scale of megawatts. Thyristors were first introduced in HVDC applications in 1970, and they have since become the heart of HVDC technology, largely eliminating the limitations of HVDC.[6] More than 100 HVDC cable systems incorporating thyristor valves have been commissioned to this day. The introduction of solid-state thyristor valves was an important breakthrough in HVDC technology, which paired with the staggering consumption and expected future demand for electricity worldwide contributed significantly to the development of HVDC technology, with a rapid increase in system voltages and capacities. In particular, countries with growing populations and rising major economies like India and China look at HVDC technology as a solution to the need for meeting the increasing demand for electricity in urban and industrialized areas, often located far from power generating stations. The Xiangjiaba-Shanghai HVDC project is an example of how fast demand for electricity is growing in China, and how

HVDC technology has proven to be the best answer to these needs. The system operates at ± 800 kV, with a capacity of 6400 MW and it was built to export hydro power from the Xiangjiaba dam in Sichuan province, to the major city of Shanghai, over a distance of ~ 2000 km. To date, it is the largest HVDC project undertaken, and it is providing electricity to a heavy industrialized area with a population of close to 25 million people. To counter climate change and greenhouse-gas-related issues, it is also critical to seamlessly integrate electricity – produced through renewable resources like solar, wind and hydroelectric power installations – into the electrical grid. This demand drives the research of new concepts for key HVDC components. In recent years the EU has been promoting an investment in renewable energies in order to decrease greenhouse gas emissions by an estimated 80-95 % by 2050. This means that the EU must produce at least 75 % of the electricity it consumes from renewable resources by 2050.[7] HVDC systems will play a key role in the realization of this goal, with the creation of an extensive transmission network aimed at the distribution of green energy across Europe.

1.2 From gutta-percha to XLPE: evolution of High Voltage cable insulation technology

The most cost-efficient way to transport electricity is through overhead lines, where the cables are suspended from the ground and air acts as the insulation. However, this technology cannot be easily implemented when transportation over long stretches of sea or through urban areas is required. In all situations where overhead lines cannot be implemented, more complex and costly undersea and underground cable systems are used. Unlike overhead lines, undersea and underground cables require insulation and protection from the environment in order to avoid power losses to the ground. The invention of the insulated conductor can be traced back to 1830 albeit it took almost 50 years before the first underground cable for the transmission of direct current was brought into use in Berlin, in 1880. At first the material of choice was gutta-percha, a polyterpene (or specifically

trans-1,4-polyisoprene), which at the time was deemed to be the most suitable material for submarine cable insulation because the cold underwater environment improved its insulating properties. However, the material presented serious drawbacks. Gutta-percha had neither a high heat resistance nor dielectric strength, and its increase in demand towards the end of 19th century led to a collapse of the supply. The invention of a dielectric material capable of withstanding the heat of the conductor and the strength of the electric field was achieved in 1880, when Ferranti introduced a multi-layer dielectric using lapped paper tapes. In 1913 the invention was further improved by introducing the use of metallized paper, in order to limit the electrical field of the core (*radial field cable*). This allowed to increase the ionization threshold voltage and enabled the production of cables with a rated voltage of up to 60 kV. To achieve high voltages of 100 kV and above it was necessary to avoid the formation of voids in the dielectric, where partial discharge could occur at high field strengths, leading to the destruction of the insulation layer. The problem of void formation in the dielectric was solved by Luigi Emanueli, chief engineer at Pirelli in Milan, who created a *thermally stable* high voltage cable for a rated voltage above 100 kV in 1924. He developed an oil-filled paper-insulated cable, where the layered paper dielectric was impregnated with a low-viscosity medium which flowed into the expanding dielectric on heating and was forced back into reservoirs on cooling. One downside of paper insulated cables is the tendency of the oil to drain or migrate from the uphill part of the cable when laid on steep slopes. This problem was overcome with the introduction of mass impregnated non-draining cables (MIND), in which the layered paper insulation is impregnated with a non-draining resin containing petroleum jelly or waxes. Similar cables based on oil-filled paper insulation and MIND technology are still in use today for high and extra high voltage applications.

Polyethylene (PE) was introduced as a cable insulation material in 1944 in the USA and in 1966 the first high voltage cable with PE insulation was commissioned at 138 kV.[1] Single layer

insulation has several advantages over oil-filled paper insulation technology because it enables a simple, continuous production process, allows a higher operating temperature and requires less maintenance. A major breakthrough in PE insulated cables for high voltage transmission was the introduction of crosslinked polyethylene (XLPE), which allowed to overcome the low onset of melting and softening of PE, enabling the insulation to withstand elevated operating temperatures up to 90 °C. High voltage XLPE cables rated up to 400 kV have been available since 1988. Considerable research efforts are dedicated to further improvement of the polymeric insulation, given the fact that a better dielectric will ultimately allow the production of cables with higher power ratings. Several companies as well as many academic research institutes and universities are active in research and development dedicated to insulation materials.[8-18] ABB successfully tested a 525 kV DC cable system with a power rating range of up to 2.6 GW.[19] Prysmian, in Milan, is developing a new cable technology for the development of power transmission grids and has recently tested a 600 kV cable with a propylene-based thermoplastic elastomer (HPTE) insulation. Furthermore, the Danish company NKT has announced the testing of a HVDC cable rated at 640 kV that is based on XLPE insulation developed in Karlskrona, Sweden, which is currently the highest voltage rating for a single extruded HVDC cable.[20, 21] The power cables industry ultimately aims for ambitious HVDC projects that will operate at 1000 kV.[22]

CHAPTER 2

2.1 High Voltage cable design

High voltage cables share common design features regardless of the type of insulation. The components that determine the electrical and thermal behavior of the cables are the conductor, the insulation layer, the inner and outer field limiting layers and the metallic sheath (Figure 1). In the following, the design of extruded HV cables is discussed in more detail.

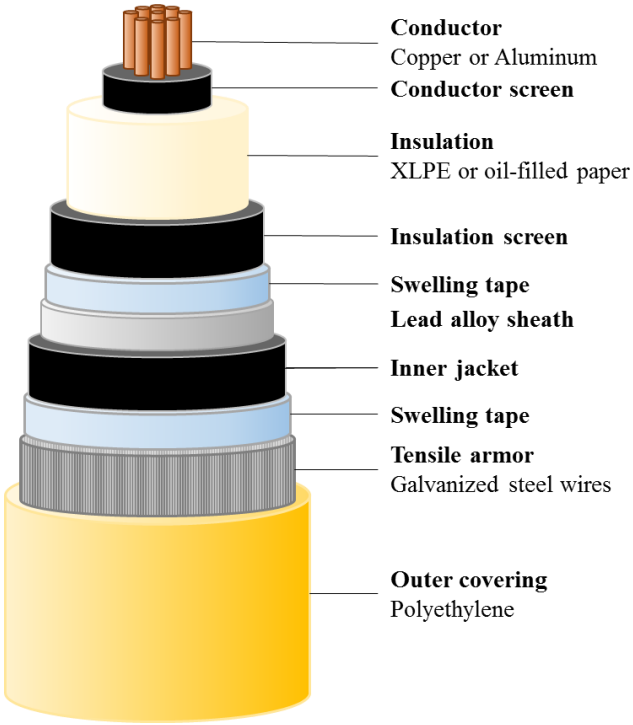

Figure 1: schematic representation of an undersea HVDC cable.

2.2.1 Conductor

The purpose of the conductor is to transmit the current with the lowest possible losses. The most common materials for HV cable conductors are copper (Cu) and aluminum (Al), with copper being more widely used due to its 60 % lower specific resistance and the resulting smaller cross-section for a given current carrying capacity. Both materials are technically viable, and selection is usually carried out on an economic basis, taking into account the higher tensile strength of copper and the

lower density of aluminum. Different conductor designs ranging from single to multi strand, round to oval and full to hollow are influenced mainly by the value of the rated current and the dielectric of choice. In the case of oil-filled cables, for example, the conductor is hollow in order to allow the impregnating medium to expand under the influence of a thermal load. An in-depth discussion of the different types of conductor designs is beyond the purpose of this thesis.

2.2.2 Field limiting layers

Field limiting or semiconductive layers constitute the interface between conductor and insulation and between insulation and metallic sheath (c.f. Figure 1). Their purpose is to ensure an even cylindrical field. These semiconductive layers ensure the equalization and reduction of the electrical stress in the cable dielectric by preventing local field enhancement through non-homogenous areas, in particular between the wires constituting the conductor or screen and the insulation. In this way, the stress enhancement by small radii single wires is eliminated leading to a cylindrical field distribution. Moreover, the presence of field limiting layers prevents the formation of voids between conductor, screen and metal sheath and the insulation layer. This is of utmost importance when the cable is subjected to mechanical stress such as bending or thermal expansion of the components at different temperatures. The presence of semiconductive layers is particularly important for polymer-insulated cables, where an impregnation medium is absent. In the case of extruded polymeric insulation, the semiconductive layers are mostly made of the same material that constitutes the dielectric layer in order to ensure a similar thermal expansion coefficient. The necessary conductivity of the semiconductive layer is reached by adding a conductive material, i.e. carbon black. To prevent the inclusion of foreign materials, high voltage cables are produced by triple extrusion, during which insulation and the two semiconductive layers are extruded over the conductor in a single process.

2.2.3 Metallic covering

Metallic coverings concentrically surround the cable core and insulation. Cable screens and metallic sheaths fulfill several tasks, including the conduction of the earth fault current in case of a cable fault until the system is switched off, the reduction of the influence of the electric field on the environment around the cable, the protection against accidental contact, and electrostatic screening. Moreover, metallic coverings act as protection from water and moisture.

2.2.4 Corrosion protection and outer covering

The most external layer of an HV cable is usually constituted of a sheath of high density polyethylene (HDPE) or polyvinyl chloride (PVC), which provides protection while laying the cable, as well as against corrosion caused by water. Sometimes, high viscosity bitumen-based compounds in conjunction with textile tapes are used as passive corrosion protection between the metal sheaths and the external HDPE layer, in order to permanently prevent any possible corrosion of the metal covering.

2.2.5 Insulation

The insulation layer is a key component of any high voltage cable. The insulation consists of a hollow cylinder of a dielectric material, or a combination of insulating materials, whose most critical parameters are a low electrical conductivity,[11, 23] low dielectric losses,[1, 24] high dielectric strength and sufficient form stability at operating temperatures.[21] The most widely used dielectrics are *impregnated multi-layer paper* and *extruded polymer* insulation. Today, extruded polymer insulation has replaced oil-filled paper insulated systems as the primary solution for HVAC cables due to a combination of lower material and processing costs, higher reliability as well as superior electrical and mechanical properties. The adoption of extruded polymeric insulation for HVDC

cables has been slower due to the low demand for such systems in the past. In recent years, however, thanks to improvements in HVDC technology and the need for long distance energy transmission, the use of extruded HVDC cables has become more attractive.[3, 21, 25] It is paramount to use a particularly clean and pure material for the insulation layer to ensure a low electrical conductivity, in order to avoid partial discharges during operation.[1, 26-28] Extruded insulation consists of polyethylene (PE), a versatile material [29]with properties that can be varied widely by tuning polymerization methods. PE is the polymerization product of ethylene, C_2H_4, which undergoes polymerization upon contact with either a catalyst or a radical initiator. This type of polymerization releases no by-products such as water or low-molecular weight hydrocarbons, and this constitutes an important prerequisite for the extraordinary good dielectric properties of PE.

With regards to HVDC, the electrical stress is primarily governed by the electrical conductivity of the insulation. *Electrical conductivity* σ is the ability of a material to conduct an *electric current* and can be broken down into a product of three terms: the carrier charge *q*, the concentration of charges *n* (number of charges per unit volume) and the charge mobility μ (the average velocity of a carrier due to an applied electric field of unit strength). Electrical conductivity plays an important role in the build-up of space charges, which can distort and locally enhance the electric field, increasing the risk of electrical breakdown.[30, 31] The total conductivity is the sum of all contributions from different types of carriers:

$$\sigma = \sum n\mu q \qquad (3)$$

Contribution to the total electrical conductivity can come from both *electronic* and *ionic charges.* *Electronic conductivity* arises when electrons (or holes) are injected into a material. Alternatively, charges can be created through promotion of electrons from the valence band (VB) to the conduction band (CB). Polyethylene displays a very low electronic contribution to the electrical

conductivity thanks to a very high band gap, which for crystalline PE is as high as 8.8 eV; therefore excitation of electrons is very unlikely.[32] However, although perfect, defect-free, crystalline polyethylene may have a high band gap, various types of imperfections can erode the electronic structure. *Ionic conductivity* describes electrical conduction due to the motion of ionic charges. Ionic conductivity is not an intrinsic property of the material but arises due to impurities. There are many different ionic charge carriers, but ionic mobility is generally much smaller than the values typically found for electrons.

The electrical properties of a given material depend on the amount of both ionic and electronic charge carriers. For polyethylene, the hole mobility along the chain is estimated to be as high as 10^{-5} cm^2/Vs,[33] which is at par with many early organic semiconductors. Chemical imperfections such as polar functional groups, catalyst residues or physical imperfections close to interfaces with other materials introduce defects in the electronic structure. Such defects can both introduce charge carriers but also act as traps, thus reducing the mobility of charges.[34] The presence of mobile impurities in the dielectric can increase *ionic conduction*, which can however be minimized by using a highly pure polyethylene grade.

The industrial process used to synthesize PE has to be taken into account when choosing the right material grade for HV insulation. The most common grades of polyethylene produced on an industrial scale are low density and high density polyethylene. In case of HDPE the polyethylene chain is linear and there are no long chain branches (LCBs). This linear structure gives rise to a high degree of crystallinity of up to 80 %, and a density of up to 0.97 $g \cdot cm^{-3}$. On the contrary, LDPE entails both long (LCBs, 1-2 per 1000 carbons) and short chain branches (SCBs, 10-50 per 1000 carbons), which hinder crystallization and lead to a material with an overall crystallinity of 30-55% and a density of ~ 0.92-0.94 $g \cdot cm^{-3}$. This difference in polymer constitution leads to a significantly different melting behavior.

LDPE features a broad melting endotherm with a peak T_m ~ 110 °C, while HDPE presents a narrower melting endotherm with a T_m ~ 130 °C. Thanks to its higher melting temperature, HDPE insulated cables would be able to sustain higher operating temperatures. However, HDPE is synthesized through Ziegler-Natta catalysis:[35-37] this polymerization technique necessitates the use of metal catalysts and co-catalysts, which are difficult to remove from the polymer, and are thought to affect the ionic conductivity of the material. Instead, LDPE can be polymerized at high pressure without the need for catalysts, and its purity makes it the material of choice for HV cable insulation. During polymerization, the reaction between ethylene monomers is initiated by the presence of a small amount of oxygen in high pressure tubular reactors operated at 200 °C and 1500-3000 bar, leading to a highly clean and pure material.[36] However, the low crystallinity and consequently the low onset of softening and melting requires that LDPE is crosslinked in order to ensure dimensional stability at the operating temperatures of high voltage cables, ranging from 70 to 90 °C.

Complete softening above T_m is prevented once polymer chains are connected by crosslinks between the main chains, which results in a form stable material.[38] Above T_m, crosslinked polyethylene (XLPE) assumes a rubber-elastic state, rather than a fluid state. XLPE can be thermally stressed to a considerably higher degree compared to LDPE, allowing a continuous cable operating temperature of 70 °C. In a high voltage cable short-circuiting through the insulation layer may occur, resulting in excessive current flow through the "short". Short circuits can produce very high temperatures, which can lead to the destruction of the dielectric. XLPE cables can be designed for a maximum short-circuit temperature of up to 250 °C, substantially higher compared to 150 °C in case of LDPE.[1] Several agents can be used to crosslink LDPE and its copolymers, and include silanes,[38-41] azo-compounds and peroxides,[39, 40, 42] as well as treatment with e.g. β- or γ-radiation.[10, 43] For the electrical insulation of e.g. medium and high-voltage power cables, crosslinking with peroxides (R-O-O-R') is the most common process.

Peroxides are widely used because they are stable compounds until heated. Generally, the peroxide is first added to the PE compounds, and crosslinking takes place continuously during cable production. The peroxide is activated by splitting the O-O bond upon heating to T > 150 °C, thus generating R-O$^{\cdot}$ radicals. These radicals extract single hydrogen atoms from PE chains, creating PE$^{\cdot}$ radical chains, which upon recombination form the infusible, crosslinked network of XLPE.

2.3 XLPE insulated HVDC cables production

The production of XLPE insulated HV cables can be summarized in four stages: *conductor manufacturing* (wire drawing and laying up), *core manufacturing* (extrusion and crosslinking), *degassing* (removal of by-products in heat chambers) and *sheathing*.

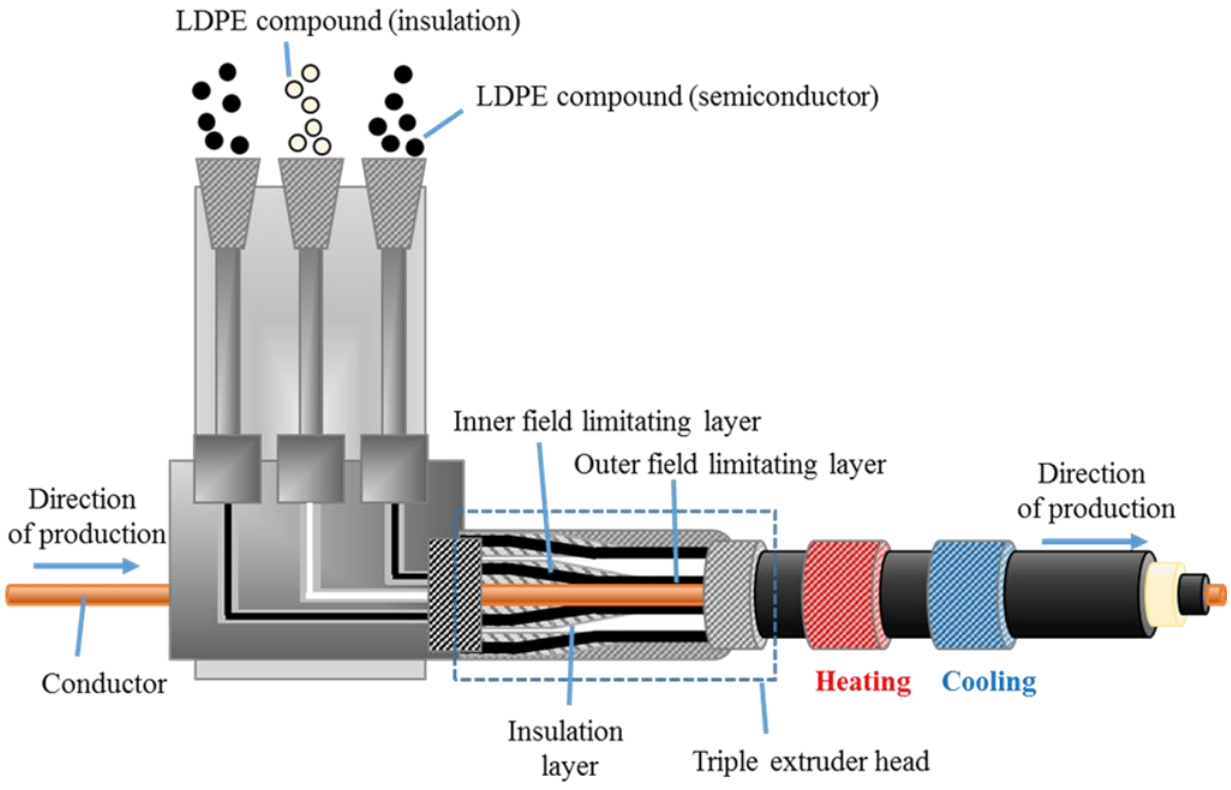

Figure 2: Schematic representation of a triple extrusion system.

Core manufacturing is the most important stage of the manufacturing process, since a good electrical stability of the extruded insulation requires a permanently strong and homogeneous bonding between the dielectric and the semiconductor field limiting layers, as well as maximum cleanliness of the material used. This process is made possible by triple extrusion, a technique introduced by Siemens in the 1960s. During this stage the dielectric, the inner and the outer semiconductor layers are extruded simultaneously onto the conductor (Figure 2). This process is a closed system, which ensures that no dust nor other unwanted material can penetrate the interfaces between the different layers.

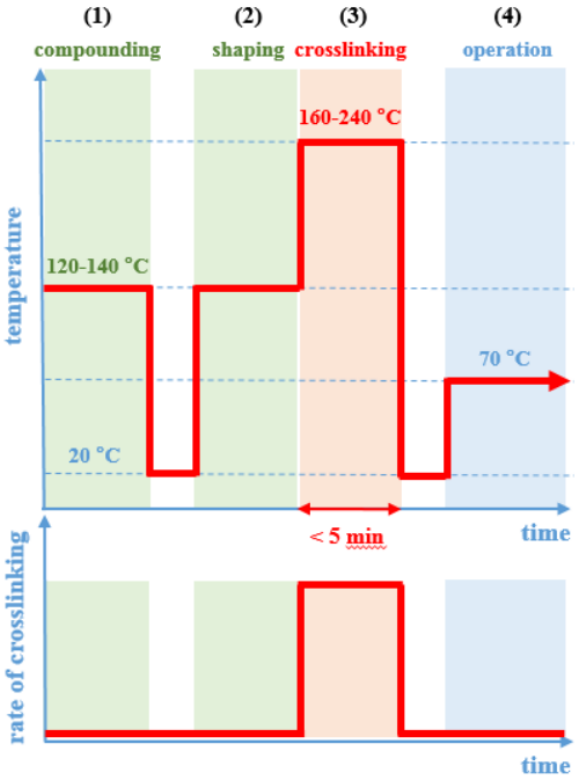

Figure 3: Illustration of the experienced temperature (top) and the rate of crosslinking (bottom) during processing (green), crosslinking (red) and operation (blue) of a high-voltage insulation material. *Reproduced with permission from the Royal Society of Chemistry (RSC).*

The conductor is usually pre-heated in order to reduce the thermal energy required during crosslinking, and to ensure a homogenous curing process also for the inner part of the insulation layer, allowing for a shorter crosslinking section and a faster production. Finally, conductor pre-heating avoids shock cooling of the molten PE upon contact with the conductor surface. Precise control of the temperature inside the extruder is critical to avoid pre-vulcanization. The temperature should be high enough to completely melt the polymer mass, but must be lower than the decomposition temperature of the peroxide used in the formulation in order to avoid pre-crosslinking. Usually, depending on the peroxide, the extrusion temperature is between 130 and 135 °C. Curing directly follows the extrusion process, when the polyethylene mass is heated to around 200 °C, which triggers peroxide decomposition and initiates the radical crosslinking (Figure 3).[40, 42] An inert gas (e.g. nitrogen, N_2) or a heat-resistant liquid (e.g. silicone oil) is used to heat the cable. Different continuous vulcanization systems can be used, each one with different advantages and disadvantages. To avoid sinking of the conductor causing eccentricity of the core (Figure 4b) low melt flow index LDPE is used, which is more viscous in the molten state and hence can bear more load.

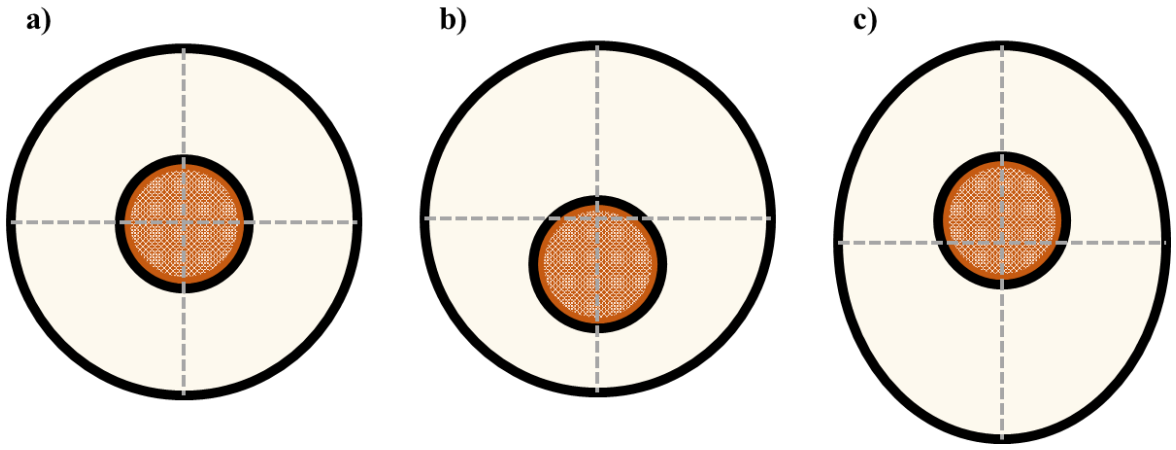

Figure 4: a) Centered **b)** Eccentric **c)** Eccentric and oval XLPE insulated cable core.

For HV cables with an insulation layer of more than a few centimeters another challenge arises from the possibility that the molten mass of polymer will drop off the freely suspended conductor, causing ovality and eccentricity of the core (Figure 4c). The use of silicon oil catenary continuous vulcanization (SiCCV) is very effective at alleviating this phenomenon, since silicon oil has a density similar to PE and compensates the gravitational effects that cause ovality of the insulation.[1] After crosslinking it is necessary to remove the volatile by-products generated by peroxide decomposition from the polymer mass. To facilitate this degassing step, cables are stored in heated chambers at 70-80 °C for several weeks (Figure 5).[44]

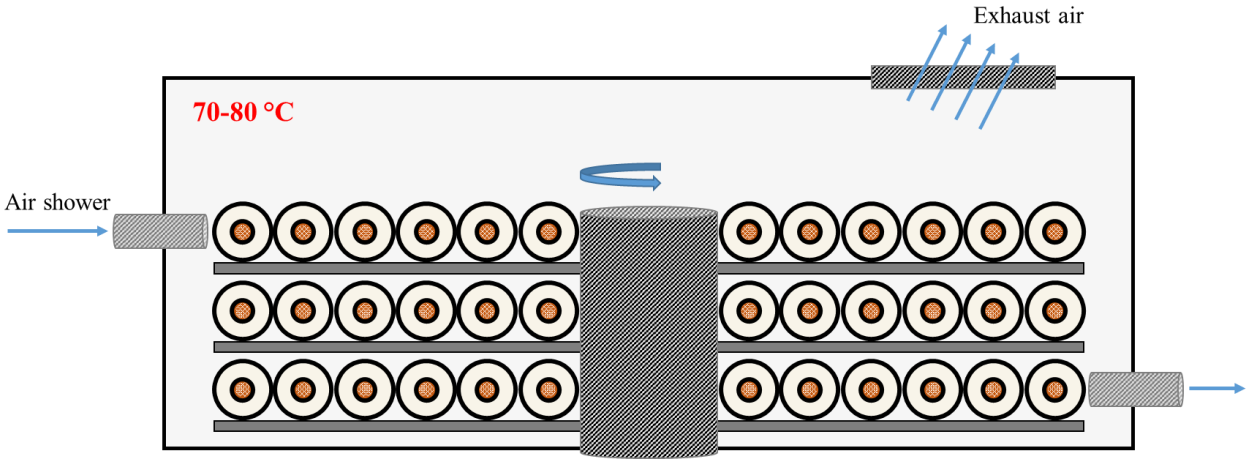

Figure 5: Schematic representation of a rotating 3-layer turntable in degassing chamber.

CHAPTER 3

3.1 Microstructure of Polyethylene

The nano- and microstructure of PE determine its physical properties, and can be described using parameters such as the crystallinity, lamellar thickness, weight average molecular weight (M_w) between entanglements and, in the case of XLPE, the degree of crosslinking and the network density. The crystallinity of PE greatly depends on the amount of SCBs and LCBs present along its polymer backbone. HDPE is mostly linear, which allows polymer chains to easily close pack and crystallize. This behavior leads to a high degree of crystallinity, which for HDPE can reach 80 %. On the other hand, LDPE is highly branched, and the presence of LCBs hinders crystallization.[45] The lamellar thickness has a strong impact on the electrical properties of polyethylene.

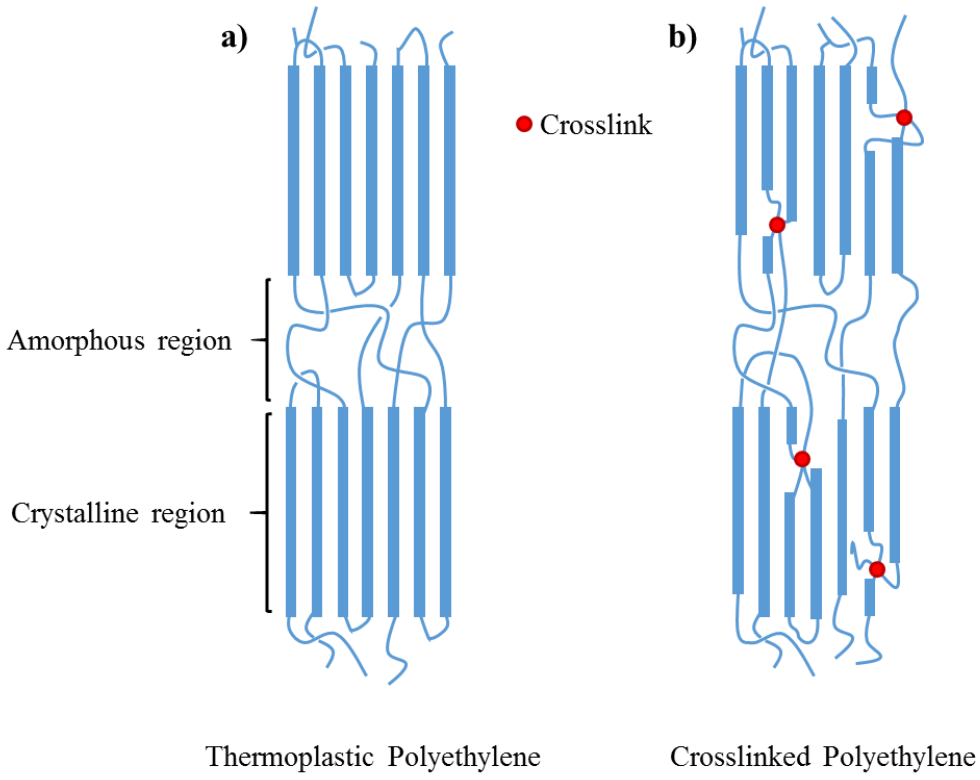

Figure 6: Principle of crosslinking of polyethylene chains.

The temperature and the rate of crystallization strongly affect the lamellar thickness: quench-cooling PE from the melt will result in thinner lamellae, while annealing at T ~ T_m will maximize the lamellar thickness. Moreover, the presence of crosslinks hinders chain folding and crystallization, reducing the lamellar thickness and the overall crystallinity of the polymer (Figure 6). The material that is not incorporated into crystals remains in amorphous regions. Lamellae are interconnected via tie chains, which are responsible for the ductility of the semi-crystalline polymer. Crystalline domains on the other hand provide the material with rigidity and a high softening temperature.

3.2 Introduction to polyolefin crosslinking

Crosslinking is a broadly used method for adjusting the properties of polymers, which involves the formation of covalent, ionic or physical bonds between polymer chains resulting in the formation of a polymer network. The resulting modification of mechanical properties depends strongly both on the polymer used and the number of crosslinks, or crosslinking density. According to IUPAC, a *crosslink* is defined as "a small region in a macromolecule from which at least four chains emanate".[46] Crosslinks form via reactions or interactions involving sites or groups on existing macromolecules. The term *curing* is used as a synonym for crosslinking of thermosetting resins such as unsaturated epoxy or polyester-based resins, while the term *vulcanization* is commonly used for rubbers such as polyisoprene and styrene-butadiene rubber (SBR), which are used for most street-vehicle tires.[47-49] A further type of thermoset materials are crosslinked polyolefins, in particular crosslinked polyethylene.[38-40, 50] Polyethylene is the most widely used thermoplastic material, and for some applications, such as HV cables, it is mandatory to modify its structure trough crosslinking in order to improve certain critical properties, e.g. its form stability and creep resistance.[38, 50]

Different procedures can be employed for the crosslinking of polyolefins, involving radical crosslinking with peroxides,[39, 40, 42, 51] grafting of silane groups, which form crosslinks via hydrolysis of silanole moieties,[39-41, 52] or high-energy irradiation either with γ-rays or electron beams.[10] Polyolefin crosslinking may be carried out either in the melt or in the solid state, depending on the curing method of choice. While crosslinking in the melt leads to a homogeneous distribution of crosslinks in the polymer network, crosslinks generated in the solid state are usually confined to the amorphous-crystalline interphase.[38, 53] Crosslinking results in distinct changes of the nanostructure of polyethylene, i.e. a decrease of the melting and crystallization temperature after curing. In the case of high voltage cables with XLPE insulation, the curing process grants the dielectric material improved thermal stability (ensuring dimensional stability at high temperatures), improved stress cracking, solvent resistance and low temperature embrittlement and weatherability (Figure 7).[40]

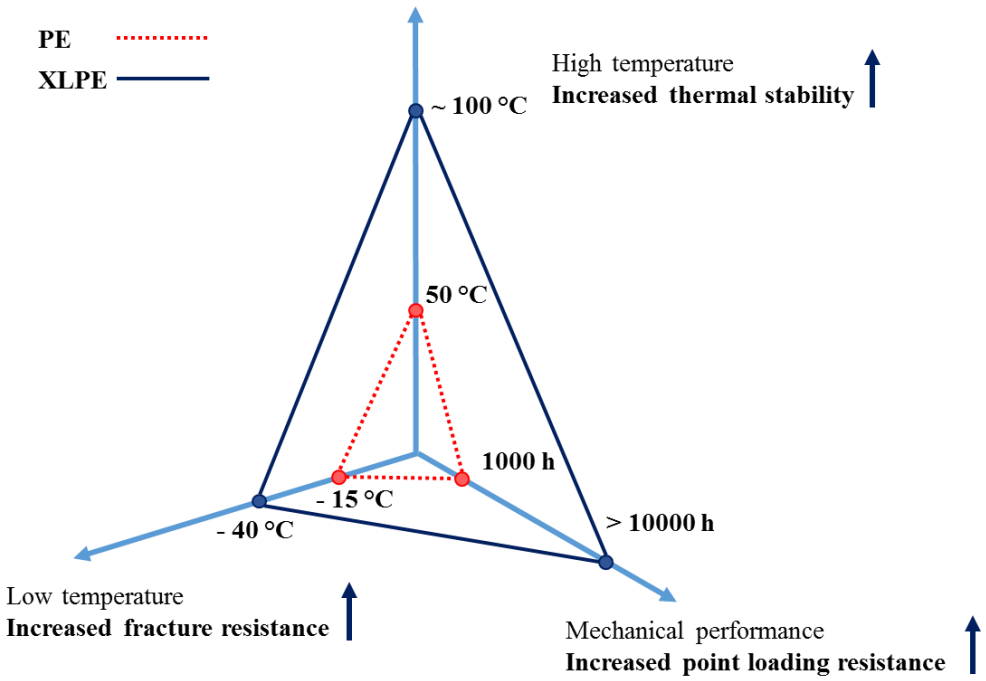

Figure 7: Improved properties of XLPE compared to thermoplastic polyethylene.

3.3 Polyethylene crosslinking with peroxides

Saturated polyolefins such as polyethylene, polypropylene (PP) and polyvinylchloride can be easily cured through radical crosslinking initiated by thermal decomposition of peroxides.[39, 40] This process involves the abstraction of a hydrogen radical from a polymer chain in order to generate a free-radical initiator site on the macromolecule. The recombination of free-radical macromolecules (two at a time, i.e. $-CH_2-\dot{C}H-CH_2-$), quickly leads to the formation of an infusible network of crosslinked polymer.[42]

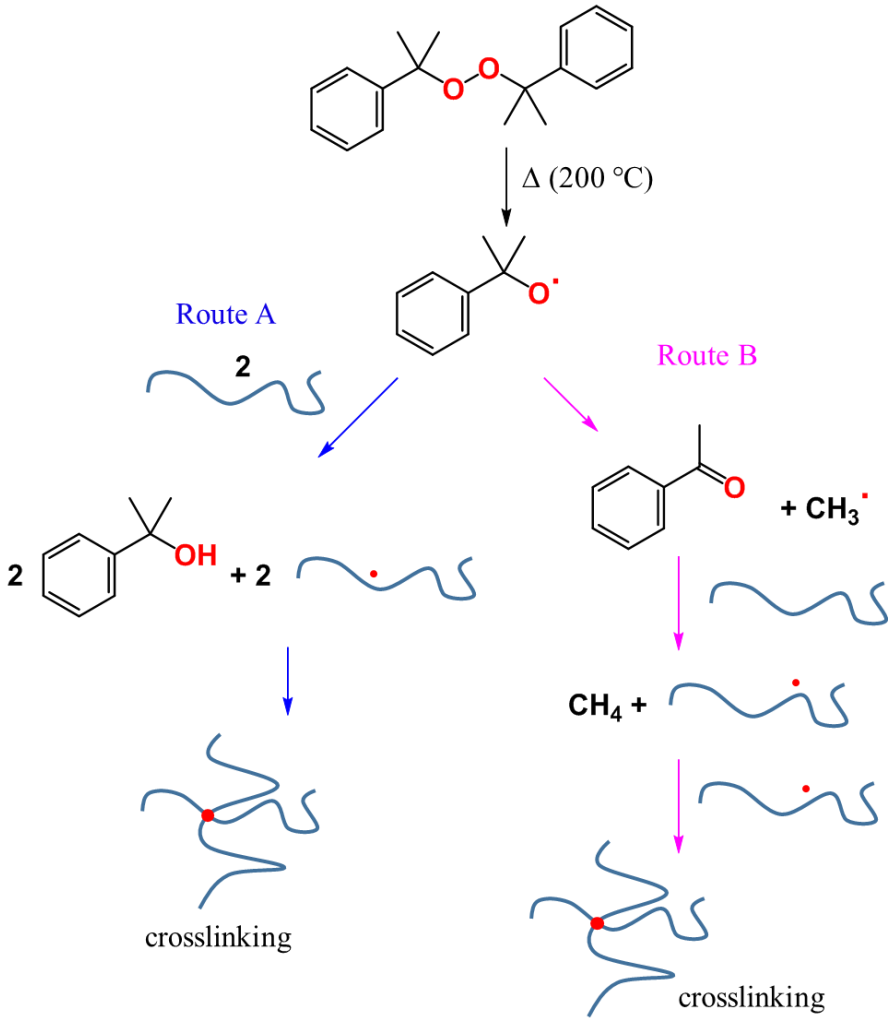

Figure 8: Stages in dicumyl peroxide decomposition and radical crosslinking of polyethylene.

The relatively high stability of peroxides at temperatures of typically less than 150 °C is key to melt processing without initiation of the curing process. Polyethylene is usually crosslinked with dicumyl peroxide (DCP): (1) first the polymer already containing the peroxide is extruded at about 130-135 °C, (2) shaped and then (3) heated at 200 °C (c.f. Figure 3), which triggers the radical decomposition of DCP and initiates PE crosslinking (Figure 8).[42] The crosslinking of PE with DCP was first accomplished by Gilbert and Precopio at General Electric.[54, 55] Dicumyl peroxide decomposes into two cumyloxy radicals Ph-C(CH_3)$_2$O$^{\cdot}$ of equal reactivity. Alkoxy radicals are strong hydrogen abstracting agents and they quickly react with the polymer chains, releasing two macromolecular free-radical initiators -CH_2-$^{\cdot}$CH-CH_2- (Route A, Figure 8).[42] Alternatively, a cumyloxy radical can undergo decomposition trough a β-scission reaction, leading to the formation of acetophenone and a methyl radical, $CH_3^{\cdot}$ (Route B, Figure 8). The methyl radical itself is a strong hydrogen abstracting agent, and will react with a polymer chain to produce a free-radical macromolecule. Considering the high reactivity of the alkoxy radicals, it is reasonable to foresee that two macroradicals will be formed close to each other and upon recombination generate a crosslink.[39, 40, 42] Apart from crosslinking, the use of dicumyl peroxide (DCP) produces a range of unwanted, low molecular weight and volatile by-products such as water, methane, acetophenone, cumyl alcohol and α–methyl styrene.[42, 44, 56, 57] Methane in particular is a flammable hydrocarbon gas, which has to be carefully removed prior to further treatment of the cable. The presence of high pressure in the vulcanization tube prevents these volatile by-products from producing bubbles and voids in the PE melt, and this pressure is maintained until the insulation layer has solidified. This procedure will also ensure that at the end of the vulcanization process the insulation will contain an approximatively constant amount of by-products throughout its thickness, reflecting the uniform distribution of DCP during extrusion. Over time, this distribution will change as by-products diffuse towards the surface.[57]

To ensure that cables are free from volatile by-products, which are known to have a detrimental effect on the dielectric properties,[9] cable manufacturers ensure that sufficient degassing is performed during the production process.[9, 44, 56] The thickness of the cable core as well as the boiling point of some by-products, in particular α-methyl styrene (T_b ~ 165-169 °C), cumyl alcohol (T_b ~ 202 °C) and acetophenone (T_b ~ 202 °C), lead to a costly and time consuming degassing process, which is carried out at temperatures between 50 and 80 °C (c.f. Figure 5).[44] Moreover, the release of e.g. α-methyl styrene represents a health hazard, and its presence requires a suitably adapted work environment. These installations consume a large amount of energy and take up considerable factory space. During degassing it is important to avoid damage to the core caused by the difference in thermal expansion of XLPE and the conductor, which can lead to undue deformation of the cable. The peroxide crosslinking efficiency of PE largely depends on the amount of terminal vinyl groups present along the polymer chain. The incorporation of comonomers such as 1,9-decadiene reduces the amount of DCP that is needed to achieve a sufficient degree of curing compared to neat LDPE. As a result, the use of unsaturated polyethylene copolymers allows to reduce the amount of volatile by-products and consequently the time of degassing.[42] In this case, two crosslinking reactions take place simultaneously: the radical polymerization of vinyl groups and combination crosslinking. Using a smaller amount of peroxide during the crosslinking process leads to a lower concentration of volatile by-products, and consequently reduces the degassing time needed to remove unwanted, low molecular weight substances that can interfere with the dielectric properties of the insulation.

3.4 Polyethylene crosslinking using silane grafting reagents

Chemical crosslinking of polyolefins can also be achieved by grafting silanes onto the polymer chains. The grafted functionalities can then function as curing agents, often in conjunction with catalysts.[41, 52, 58] The basic process involves as a first step the grafting of alkoxy-silane onto the polyethylene chain through radical grafting (Figure 9).[40, 41, 59]

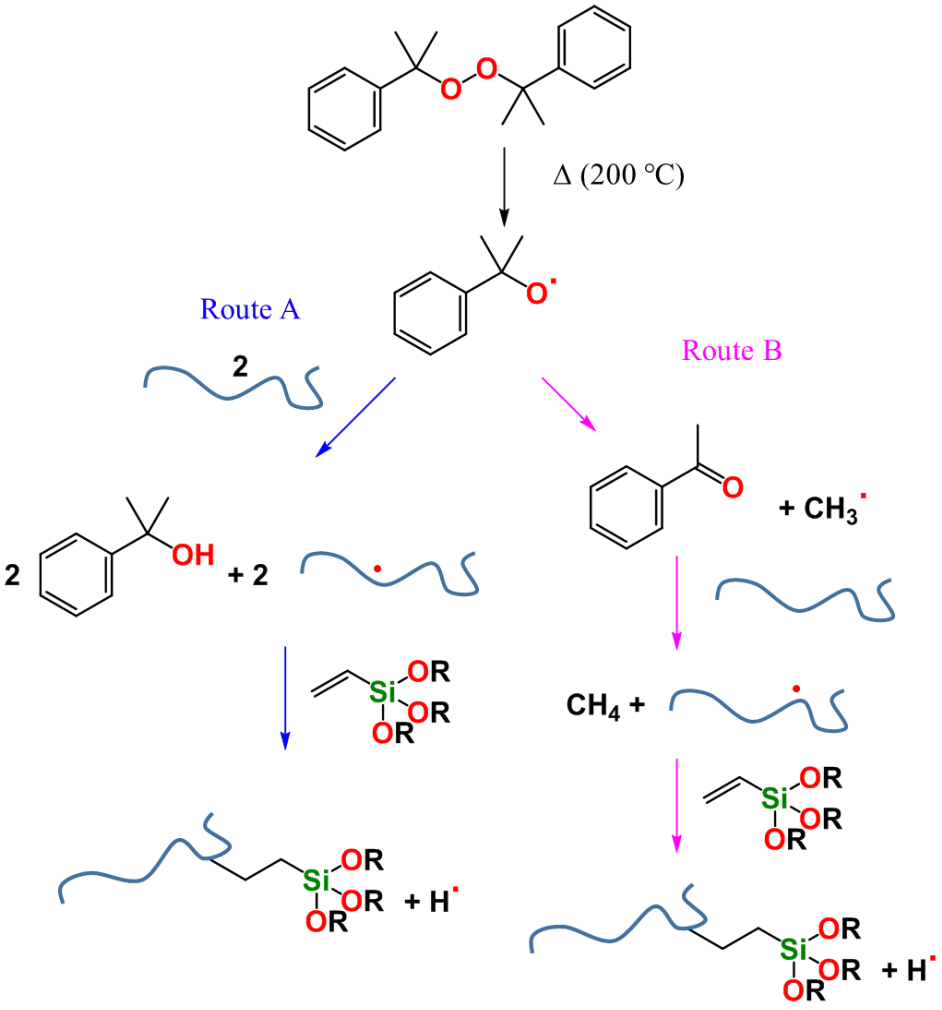

Figure 9: Radical grafting of alkoxy-silane crosslinkers onto polyethylene using DCP.

The reaction conditions of the radical grafting step are tuned in order to avoid recombination of radical macromolecules. Moreover, the molecular structure of silane reactants includes a terminal

vinyl group, which will readily react with the majority of the radicals generated by DCP.[40] Afterwards, the incorporated alkoxy groups -$(CH_2)_2$-$Si(OR)_2OR$ are hydrolyzed in the presence of water and a catalyst to release silanol groups -$(CH_2)_2$-$Si(OR)_2OH$ and ROH, which in a last step react with each other in a condensation reaction leading to the formation of a crosslinked polymer network and the release of water molecules as by-products (Figure 10).[40, 41, 52]

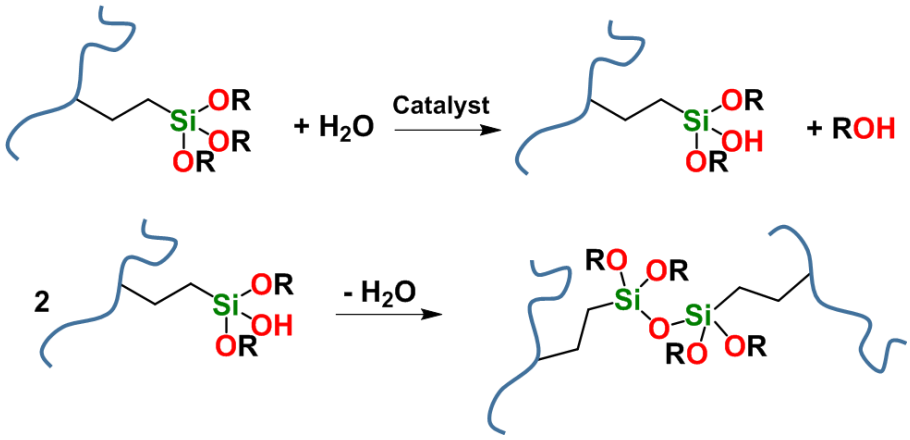

Figure 10: Catalyzed hydrolysis of alkoxy-silane, polyethylene-grafted curing agents and condensation reaction leading to PE crosslinking.

The grafting and crosslinking of polyethylene with silanes can be performed in either two separate steps or in a one-step process; both approaches rely on reactive extrusion.[40] The overall performance of silane-crosslinked PE is similar to radical crosslinked PE, but in the case of silane-crosslinking the final cured material can be tuned by the use of different alkoxy-silanes as crosslink-bridges. However, the low mobility of water through PE makes the crosslinking of thick insulation layers a slow process. Moreover, after crosslinking it is necessary to remove water and ROH molecules from the polymer mass through a degassing step. Therefore, the long processing times and the release of volatile by-products prevent the use of silane crosslinking for HV cable insulation.

3.5 Radiation crosslinking of polyethylene

Crosslinking of polyethylene can also be achieved using high-energy irradiation with X-rays, γ-rays or an electron beam.[10, 60-64] The energy carried by X-rays, γ or β-radiations exceeds the energy required to break chemical bonds. The irradiation of polyethylene leads to the formation of hydrogen and alkyl free radicals of the structure $-CH_2-\dot{C}H-CH_2-$ (by breaking a C-H bond along the polymer chain). When two such free radicals are formed on adjacent chains, a recombination reaction occurs with the formation of a crosslink between the macromolecules. Although the chemical bond strength of the C-H bond is greater compared to that of a C-C bond, chain scission (i.e. breaking of the C-C bonds along the polyethylene chain)[65] is low compared to chain recombination,[40, 61] which makes polyethylene a good candidate for radiation crosslinking. H_2 is released as a by-product of radiation crosslinking together with a small amount of low molecular weight hydrocarbons such as methane, ethane and propane.[40, 61] For electrical cables, these volatile by-products must be removed via degassing. In January 1957, Paul Cook founded Raytherm Wire and Cable (today known as Raychem) to take advantage of electron beam induced crosslinking of PE. Due to the limited penetration depth of electron beams, this technique is not suitable for crosslinking of thick insulation layers. However, radiation crosslinking is used for thinner cables, e.g. in the automotive industry.

3.6 A future approach to polyethylene crosslinking for high voltage cables

As previously discussed, polyolefins can be cured by either radiation, radical or silane crosslinking. The characteristics of the thermoset depend on the crosslinking method (Table 1).[61] Each method has its specific drawbacks when used for high voltage power cable insulation. β-radiation crosslinking is limited by the small penetration depth, and therefore is not suitable for curing of thick insulation layers.[10] Furthermore, low molecular weight by-products such as hydrogen and

methane are generated, which must be removed by degassing. Silane crosslinking is limited by the low mobility of water through PE, and the release of polar by-products worsen the dielectric properties of the material. Both radiation and silane crosslinking take place below the melting temperature T_m of polyethylene, and consequently the crosslinks are preferably formed in amorphous domains. Instead, peroxide crosslinking is carried out above the T_m of polyethylene, thus leading to a more homogeneous network.[40] However, as extensively described in section 3.3, the formation of volatile by-products requires an energy intensive and time consuming post-curing degassing step.

Physical property	Crosslinking method		
	β-Radiation	Peroxide	Silane grafting
Max gel content (%)	~70	~90	~60
Physical properties at 60 % gel			
Elastic modulus at 190 °C (MPa)	0.24	0.2	0.14
Crystallinity after crosslinking	69	60	69
Tenacity at break at 190 °C (MPa)	0.75	0.7	0.9
Elongation at break at 150 °C (%)	220	240	190

Table 1: Comparison of physical properties of HDPE crosslinked by different crosslinking methods.[61]

Click chemistry type curing of polyethylene resins bearing various functional groups promises to be an appealing alternative. *Click chemistry* was introduced as a term for the first time in 2001 by the American chemist K. B. Sharpless to classify organic reactions that (1) release only harmless or no by-products at all and (2) have a high yield.[66] Several types of reactions that fulfill these criteria have been identified, including nucleophilic ring-opening of epoxides and aziridines, non-aldol type carbonyl reactions, additions to carbon-carbon multiple bonds and cycloaddition

reactions.[17, 66-69] Thanks to their flexibility in the choice of the nucleophilic agent and the absence of volatile by-products, click-chemistry ring-opening reactions are of particular interest for the crosslinking of functionalized polyethylene resins.[16-18, 70] Epoxy-functionalized polyethylenes have received increasing attention lately, but the use of epoxy chemistry for curing has not yet been extensively studied. Epoxy ring-opening reactions for the crosslinking of polyethylene copolymer resins are the main focus of this thesis as the author believes that this kind of chemistry can represent a solution to many of the drawbacks of other polyethylene curing methods (Table 2).

Crosslinking method		**Radiation**	**Peroxide**	**Silane grafting**	**Click-chemistry**
Applications		Wires and cables, tubes, pipes, films	Wires and cables, tubes, pipes, foams	Wires and cables, tubes, pipes	Wires and cables, tubes, pipes, films
Polymer	Polyethylene	■	■	■	●
	Polypropylene	■	●	●	●
	PVC	■	●	●	x
	Engineering plastic	■	x	x	x
Capital investment		High	High	**Low**	High
Degasasing step post-crosslinking		Yes	Yes	Yes	**No**
Cost of raw materials		**Low**	**Low**	Slightly high	Slightly high
Cost of compounding		**Low**	Medium	High	**Low**
Process flexibility		**Very good**	Poor	**Very good**	**Very good**
Product thickness restrictions		< 10 cm	> 0.3 mm	> 0.3 mm	-
		Limited by penetration depth of radiation	Difficult to achieve big diameters because of output	Thickness limited by speed of crosslinking	Thickness limited by speed of crosslinking
Rate of crosslinking		**High**	Low	Low	Low
Degree of crosslinking		Medium	**High**	Low	**High**
Scrap rates		-	**High**	Low	-
Other advantages		**Clean process**	Energy intensive	**Recyclability**	**No by-products**

Table 2: Technological comparison of industrial polymer crosslinking methods. (■) In practical use (●) Technically viable, but no practical example (x) Hard to apply.

CHAPTER 4

4.1 Epoxy ring-opening reactions

An epoxide is a three-atom ring forming a cyclic ether. This ring approximates an equilateral triangle, which makes the epoxide strained and thus highly reactive. A compound containing the epoxide functional group can be called an epoxy, epoxide or oxirane, and they are industrially produced on a large scale for many applications. In particular, oxirane compounds are the key components of epoxy resins. Crosslinked epoxides exhibit outstanding mechanical properties, high adhesion strength, good heat resistance and high electrical resistance, which makes them the material of choice for many applications ranging from coatings to adhesives and matrices for fiber-reinforced composites.[71] Low molecular weight molecules or polymers bearing multiple epoxy groups can be crosslinked by reaction with curing agents such as amines,[17, 72-76] phenols,[18, 77, 78] thiols,[67, 79, 80] hydrazides,[81, 82] isocyanates or acids.[16, 83] The final properties of cured epoxy resins are affected by the type of epoxy resin, curing agent and the curing process. All these are high yield reactions that involve the opening of the strained epoxy ring without emission of volatile by-products, and they are consequently classified as click-chemistry type reactions.[66]

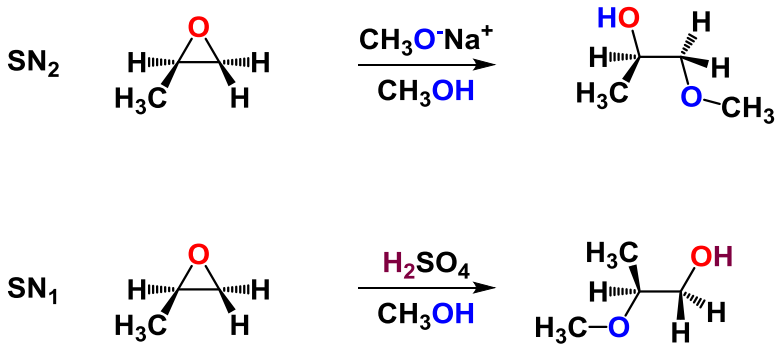

Figure 11: Epoxy ring opening reactions, SN_1 and SN_2.

Epoxy ring-opening reactions can proceed by either SN_2 or SN_1 mechanisms, depending on the nature of the epoxide and on the reaction conditions. If the epoxide is asymmetric, the structure of the product will vary depending on the dominating reaction mechanism (Figure 11).

When an asymmetric epoxide reacts in basic conditions, ring-opening occurs by an SN_2 mechanism, and the nucleophilic attack takes place at the less substituted carbon atom. Since there is no acid available to protonate the oxygen prior to ring opening, the leaving group is an alkoxide anion. The alkoxide anion is a poor leaving group, and therefore the epoxy ring is unlikely to open without the attack of a strong nucleophile. When a nucleophilic substitution reaction involves a poor leaving group and a strong nucleophile, it usually proceeds by an SN_2 mechanism (Figure 12).

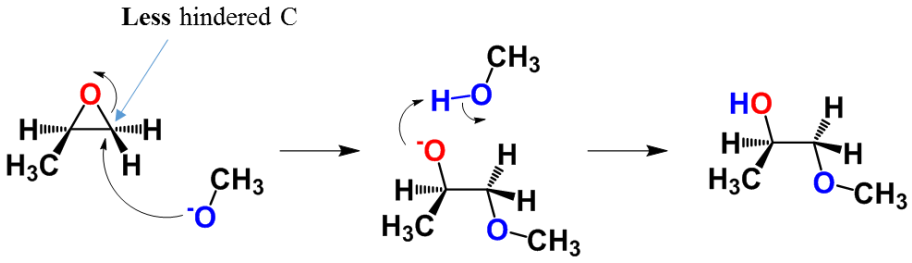

Figure 12: Mechanism of base catalyzed SN_2-type epoxy ring opening reaction in the presence of a strong nucleophile.

In case of an acid-catalyzed epoxy ring-opening reaction the first step is the protonation of the oxygen atom. This leads to the formation of a hydroxyl functionality, which is a good leaving group. Afterwards, the carbon-oxygen bond involving the more substituted carbon begins to break, and a positive charge begins to build up on the carbon atom (more substituted carbocations are more stable). Similar to an SN_2 reaction mechanism, the nucleophilic attack takes place preferentially on the less hindered face because the carbon-oxygen bond is still to some degree in place, and the steric hindrance from the oxygen blocks attack from its side (Figure 13).[84]

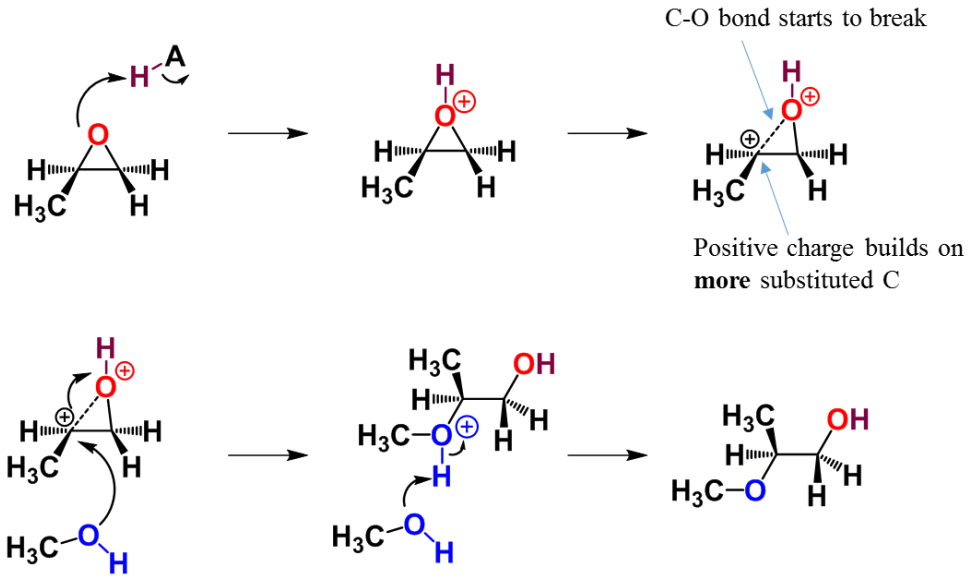

Figure 13: Mechanism of acid catalyzed SN_1-type epoxy ring opening reaction in the presence of a weak nucleophile.

The regiochemical outcome is however different from the base-catalyzed reaction: in the acid-catalyzed process, the nucleophile attacks the more substituted carbon because it is this carbon that holds a greater degree of positive charge. In contrast, in the base-catalyzed reaction the nucleophilic attack takes place on the less hindered carbon atom.

4.2 Polymerization chemistry of epoxy functional groups

The high reactivity of the epoxy group is characterized by its affinity towards both nucleophilic and electrophilic species. As a result, epoxy rings are receptive to a wide range of crosslinking agents. It is the combination of epoxy resin and crosslinking agent that leads to the cured thermoset epoxy resin, converting the initially low molecular weight reactants into a thermoset. The curing agents used to crosslink epoxides can be classified as either hardeners or catalysts, and reactants bearing epoxy rings will undergo different polymerization mechanisms depending on the nature of the curing agent of choice.

4.2.1 Epoxy step-growth polymerization

Step-growth polymerization proceeds via a step-by-step succession of individual reactions between an epoxy ring and a suitable reactive site such as an amine, phenol, thiol, isocyanate, acid or hydrazide.[71, 84, 85] Each reaction step creates a new covalent bond between a pair of functional groups. The main parameters that control the final polymer structure and properties are the nature of the reactants, the molar ratio between reagents and the number of reactive sites per monomer or polymer chain. In order to obtain a crosslinked polymer network at least one of the reactants must have a functionality of more than two (Figure 14d), since a reactant bearing a single functionality would interrupt the polymer growth (Figure 14a).

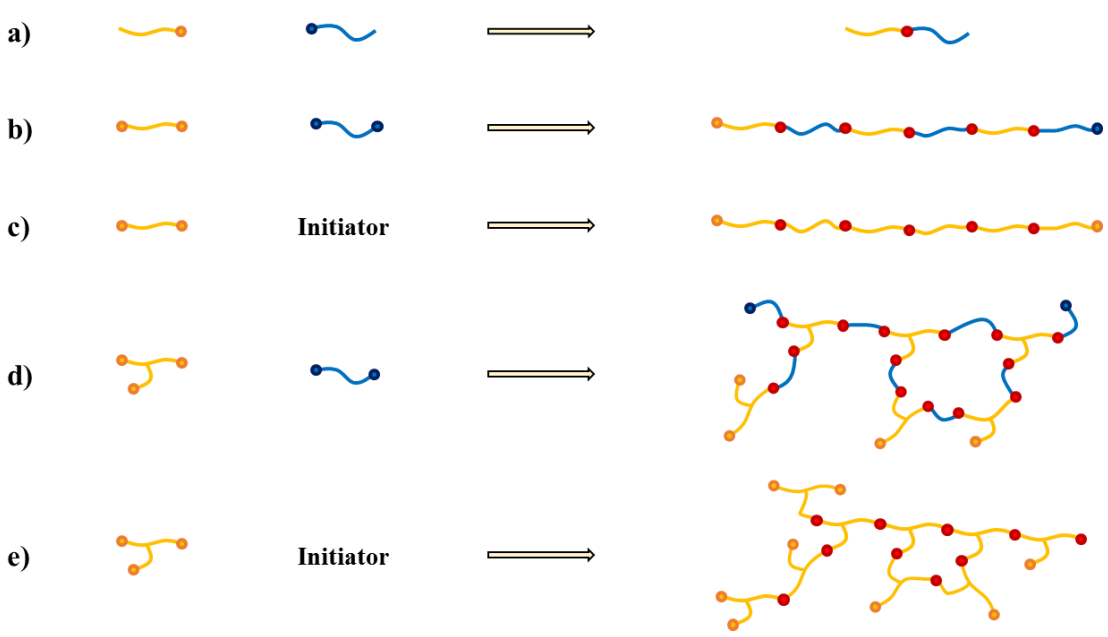

Figure 14: Schematic representation of **a)** a simple reaction between monofunctional molecules, **b)** a step growth copolymerization, **c)** an homopolymerization **d)** a step growth copolymerization where at least one monomer has more than two functionalities, generating a crosslinked network and **e)** a step growth homopolymerization where the monomer has more than two functionalities, generating a crosslinked network.

Instead, a reaction between bifunctional reactants would lead to a linear polymer (Figure 14b). These reactions can be exploited in order to crosslink macromolecules such as epoxy-functionalized PE, either by using a bi- or multifunctional low molecular weight curing agent (Figure 15a,b) or another suitably functionalized polymer (Figure 15c). Common examples of hardeners are aliphatic and aromatic amines, and carboxylic anhydrides. These compounds react directly with the epoxy rings, and therefore the epoxy resin to hardener ratio usually ranges from 3:1 to 10:1, by weight.

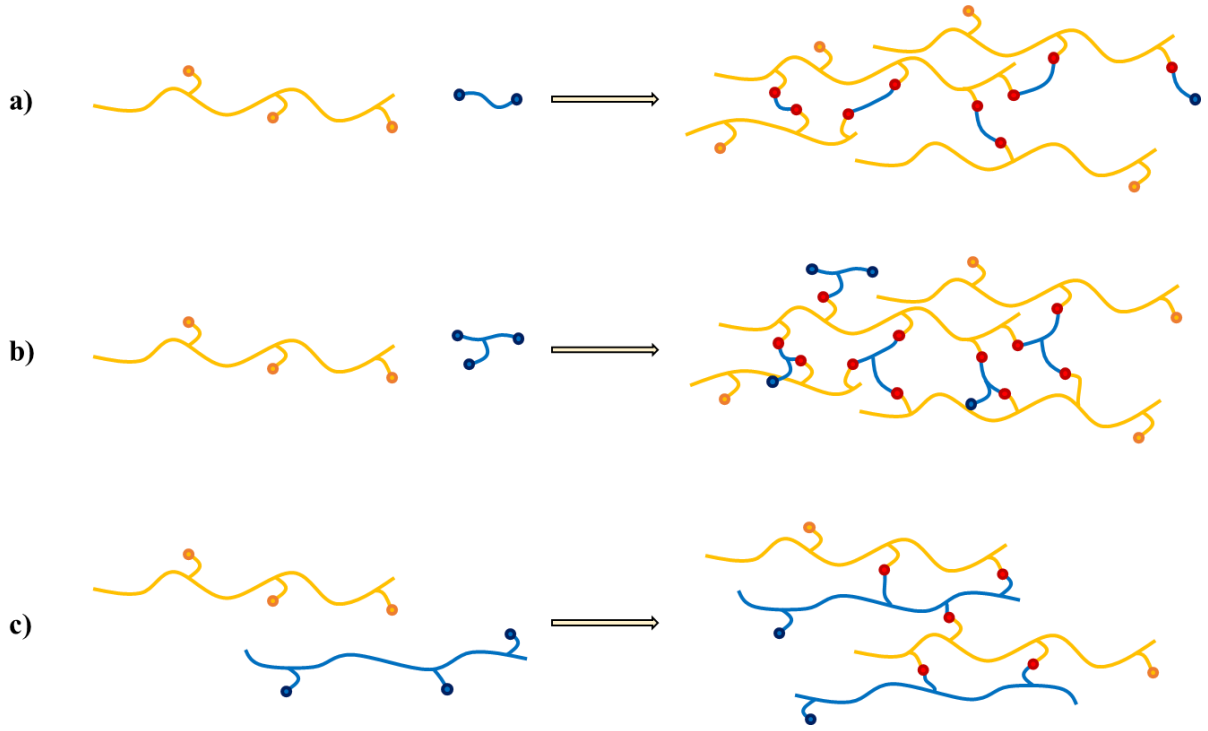

Figure 15: Schematic representation of **a)** a multifunctionalized copolymer reaction with a bifunctional or **b)** multifunctional small molecule; both reactions generate a crosslinked network. **c)** Reaction between two multifunctionalized copolymers, again generating a crosslinked network.

Amines are the most commonly used curing agents for epoxy resins. When the concentration of N-H groups equals or is higher than the concentration of epoxy rings no side reactions take place. The epoxy-amine system is therefore suitable for the synthesis of model networks. In general, amine-

based curing agents must have more than two N-H groups in a molecule in order to lead to a crosslinked polymer network. Amine reactivity increases with its nucleophilic character: aliphatic > cycloaliphatic > aromatic. Thanks to this difference in reactivity it is possible to tune the processing conditions by selecting different types of hardeners. Aliphatic amines are usually chosen for room temperature curing systems,[58] while aromatic amines find use in composite materials. Both primary and secondary amines react with epoxy rings, with primary amino hydrogens being more reactive compared to secondary ones (Figure 16).[58, 84, 86]

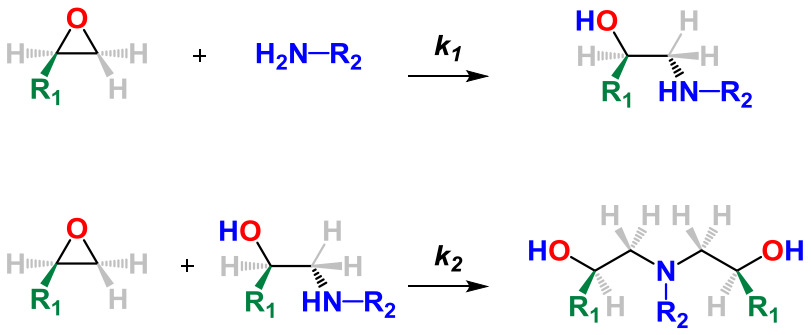

Figure 16: Epoxy-amine reactions.

When epoxy functional groups are present in excess compared to amino hydrogens, or in case the secondary amino hydrogens present a very low reactivity or steric hindrance, a side reaction between the hydroxyl groups generated by previous epoxy ring-openings and oxirane rings can become competitive, leading to the formation of an ether (Figure 17).

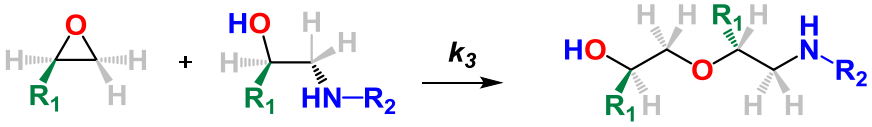

Figure 17: Epoxy-hydroxy reaction (etherification).

4.2.2 Epoxy chain homopolymerization

Epoxy rings can react with both nucleophilic and electrophilic species, thus both Lewis acids and bases are able to act as catalysts and initiate epoxy homopolymerization with a chain-growth mechanism. Depending on the number of functionalities present on the epoxy bearing molecule, different networks from linear (Figure 14c) to crosslinked (Figure 14e) can be generated. Typically, catalysts are used in low concentrations, i.e. less than 1 % by weight. Bases such as tertiary amines, imidazoles and ammonium salts initiate anionic epoxy homopolymerization, a complex reaction that is characterized by long induction periods and slow reaction rates, alongside short primary chains due to the high rate of chain transfer reactions. The addition of a Lewis acid or base to epoxy-amine or epoxy-phenol formulations accelerates the curing, but the chemistry of the process becomes more complicated due to the competition between chain-growth and step-growth polymerization mechanisms, which occur simultaneously.

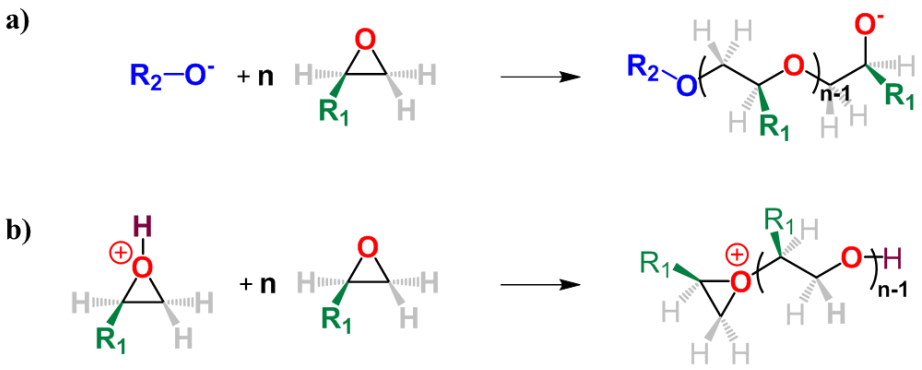

Figure 18: Epoxy chain homopolymerization catalyzed by **a)** strong base and **b)** strong acid.

Epoxy chain homopolymerization can be classified as a click-chemistry type reaction, considering the usually high yields and the absence of by-products. Depending on the catalyst, epoxy homopolymerization proceeds through an alkoxide (anionic polymerization, Figure 18a) or an ozonium (cationic polymerization, Figure 18b).

4.2.3 Epoxy chain copolymerization

Another possible polymerization mechanism involving epoxy rings is alternating chain copolymerization. The networks generated by these reactions differ depending on the number of functionalities carried by the components of the resin. Low molecular weight components with only two functionalities will lead to a linear polymer (c.f. Figure 14b), while the presence of at least one component with a higher number of functionalities will generate a crosslinked polymer network (c.f. Figure 14d). While reactions between carboxylic acids and epoxy rings follow a step-growth polymerization mechanism, Lewis base catalyzed reactions with cyclic anhydrides take place through a chainwise copolymerization.

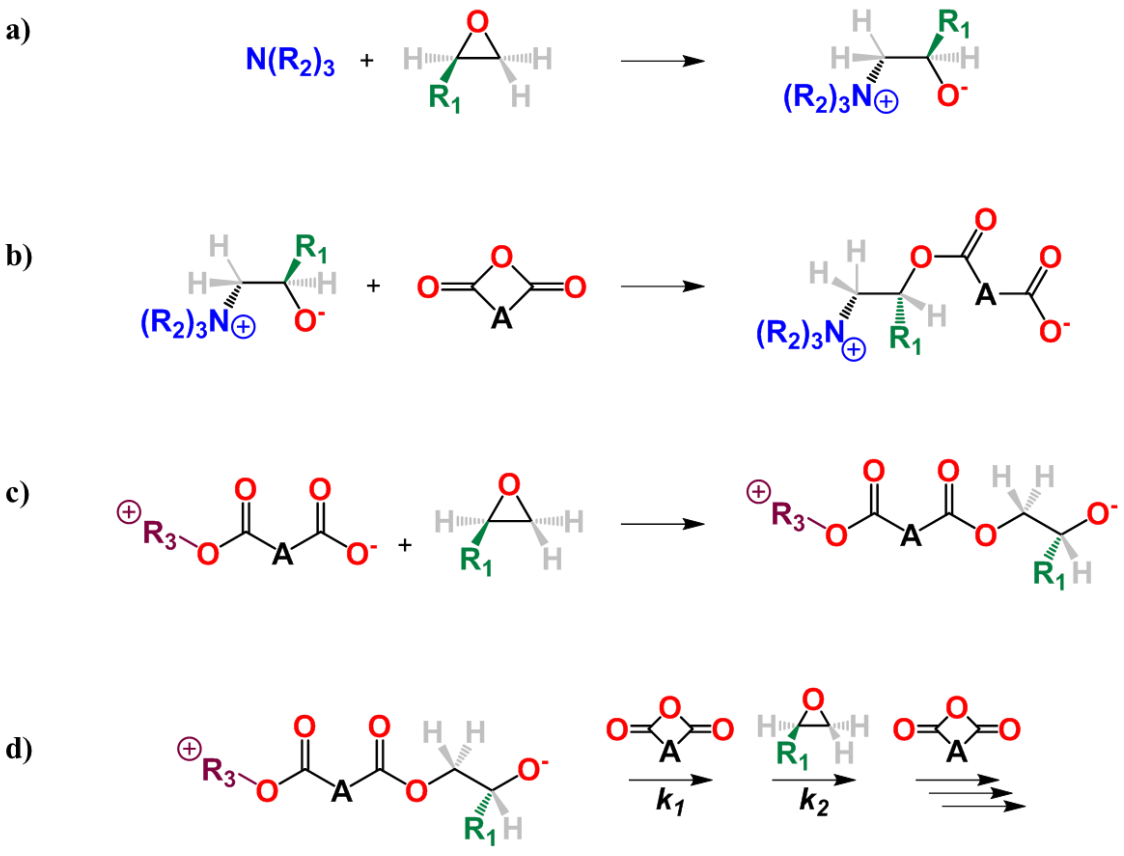

Figure 19: Epoxy-anhydride chain copolymerization mechanism.

Epoxy rings quickly react with Lewis bases such as tertiary amines, leading to the formation of a zwitterion containing an alkoxide anion and a positive charge, whose nature depends on the Lewis base used (a quaternary nitrogen in the case of tertiary amines, for example Figure 19a). The alkoxide anion reacts immediately with an anhydride group, giving rise to a species containing a carboxylate anion as reactive functional group (Figure 19b). A reaction between the carboxylate anion and an epoxy ring generates a monoester bond and leads to the regeneration of an alkoxide anion (Figure 19c), which, since $k_2 >> k_1$, quickly reacts with an anhydride regenerating the carboxylate thus propagating the reaction with an alternating chain copolymerization mechanism (Figure 19d).[87]

CHAPTER 5

5.1 Crosslinking with epoxy ring-opening reactions

The development of a byproduct-free curing process would significantly broaden the scope of polyethylene-based insulation materials. Through the incorporation of functional comonomers along the polyethylene chain it is possible to take advantage of click-chemistry type of reactions, such as epoxy ring-opening, that generate chemical bonds and crosslink the material. The focus of this thesis is to explore the viability of click-chemistry type curing of a branched statistical ethylene-glycidyl methacrylate copolymer with a comonomer content of 8 wt%, p(E-*stat*-GMA$_8$), a material widely employed as a reactive compatibilizer for polymer blends (Figure 20).[73, 88-91]

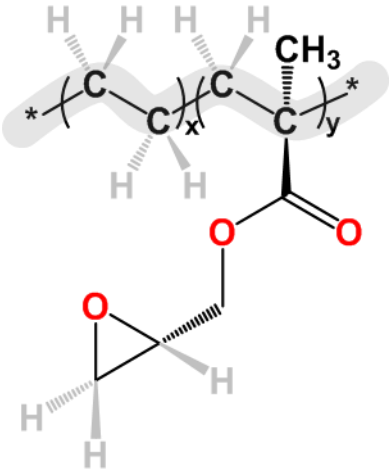

Figure 20: Poly (Ethylene-*stat*-Glycidyl Methacrylate) with a GMA content of 8 wt%, p(E-*stat*-GMA$_8$).

The epoxy groups of the GMA comonomers can react with a variety of bifunctional curing agents including aromatic and aliphatic di-amines,[17, 92] di-carboxylic acids,[93, 94] di-hydrazides[81, 95] and bisphenols.[18, 96] The efficiency of the crosslinking process strongly depends on the chemical nature of the curing agent and its stoichiometry with respect to the amount of GMA comonomer, the temperature and the curing time.

5.2 p(E-*stat*-GMA$_8$) crosslinking with low molecular weight multifunctional curing agents

The resin/curing agent must fulfil several requirements. First, it must be possible to compound and shape the resin at typical extrusion temperatures between 120 and 140 °C without occurrence of the crosslinking reaction (c.f. Figure 3). Further, the crosslinking reaction must be rapid at more elevated temperatures, typically between 160 and 240 °C, in order to generate an infusible network within a short period of time. Further, suitable curing agents must be non-toxic, liquid at the extrusion and curing temperatures, bear two or more reactive sites and have the ability to react quickly with an epoxy ring without releasing any volatile by-product.

5.2.1 Aromatic amine-based curing agents

Several aliphatic and aromatic diamines fulfill the above-mentioned requirements. The nucleophilicity of the specific amine dictates its reactivity with epoxy rings, where aliphatic amines > cycloaliphatic amines > aromatic amines. Accordingly, aliphatic amines react quickly with oxirane rings providing curing of epoxy resins even at room temperature, while aromatic amines usually require elevated temperatures. This is because the lone pair on the nitrogen atom, which is free in an alkyl amine, is present in conjugation with the aromatic core, e.g. a benzene ring in case of aniline, and hence lacks the ability to use its electron pair as easily as an alkyl amine. A primary amine has two active hydrogens that are each capable of reacting with an epoxy group. Once the first reaction occurs, a secondary amine is generated, which will react with another epoxy group. The reaction rate of the secondary amine with an epoxy resin is much slower than that of a primary amine. A second reaction will generate a tertiary amine, which has no active hydrogens. A tertiary amine will not react with epoxy resins but can contribute to the curing by catalyzing epoxy homopolymerization. Tertiary amines also accelerate the reaction between primary and secondary amines and epoxy resins.

I chose to study two non-toxic, low melting point primary aniline type compounds featuring different degrees of steric hindrance, namely 4,4′-methylenebis(2,6-diethylaniline) (MDA) and 4,4′-ethylenedianiline (EDA) (Figure 21).

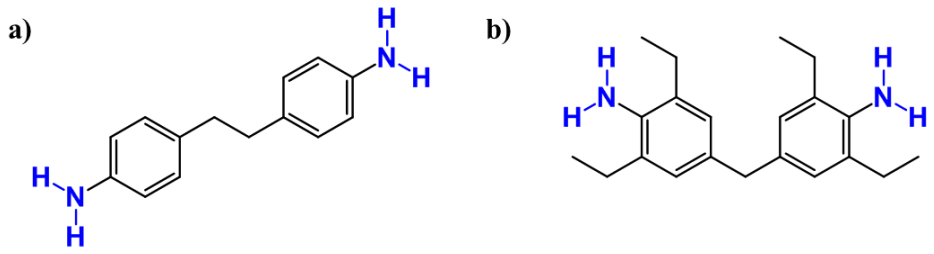

Figure 21: The aromatic amine-based crosslinkers object of this study: **a)** 4,4′-Ethylenedianiline (EDA), **b)** 4,4′-Methylenebis(2,6-diethylaniline) (MDA).

In a first set of experiments I evaluated the crosslinking efficiency of p(E-*stat*-GMA_8) with 1 wt% curing agent. Initially, I cured p(E-*stat*-GMA_8) formulations at different temperatures for 2 hours, and calculated gel content and hot set elongation ε_{hot} of the specimens according to the methods reported in Papers I-IV. The same approach has been used for the characterization of all other formulations that are discussed in this thesis. I concluded that the reactivity of MDA was too low to be of interest, since an acceptable gel content and consequently a sufficient network density could be achieved only at very high temperatures of at least 260 °C and after two hours of curing (Figure 22).

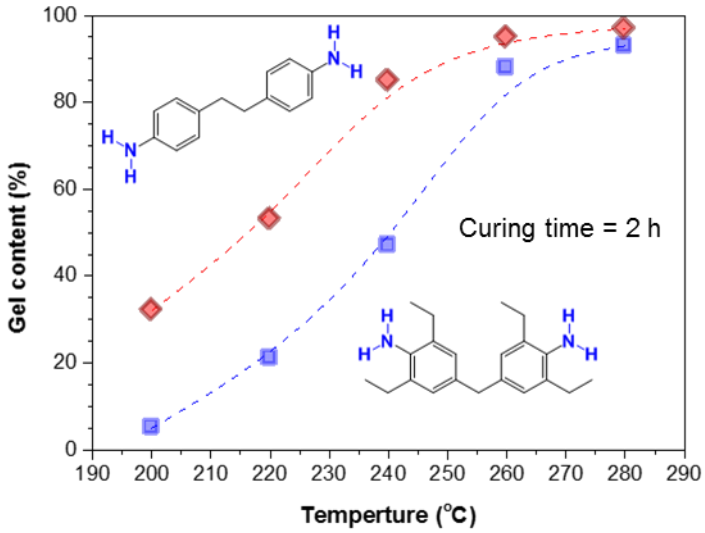

Figure 22: Gel content measurements for p(E-*stat*-GMA_8) resin cured with 1 wt% MDA (■) and 1 wt% EDA (■) at different temperatures for 2 hours.

This low reactivity can be explained taking into consideration the aromatic nature of MDA and the substantial steric hindrance generated by the ethyl groups in ortho-position (Figure 23).

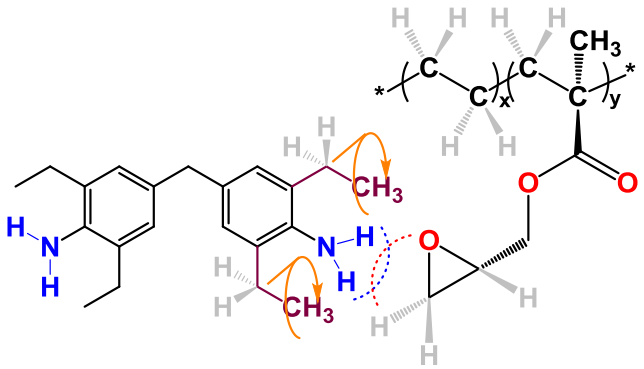

Figure 23: The steric hindrance of the two MDA ethyl groups in ortho-position complicates the approach to the oxirane group, and hence the epoxy ring-opening reaction.

Instead, EDA more rapidly leads to a high gel content; for instance, a high gel content of ~ 80 % and 90 % was reached already after 20 minutes at 240 °C using 1 or 2 wt% EDA, respectively (Figure 24). Industrial standards for electrical insulation demand a hot set elongation of ε_{hot} < 75 % for a stress of σ = 0.2 MPa,[97] which was reached only after 40 minutes of curing for 1 wt% EDA. Doubling the EDA content greatly increased the crosslinking speed, leading to an ε_{hot} < 50 % already after 20 minutes.

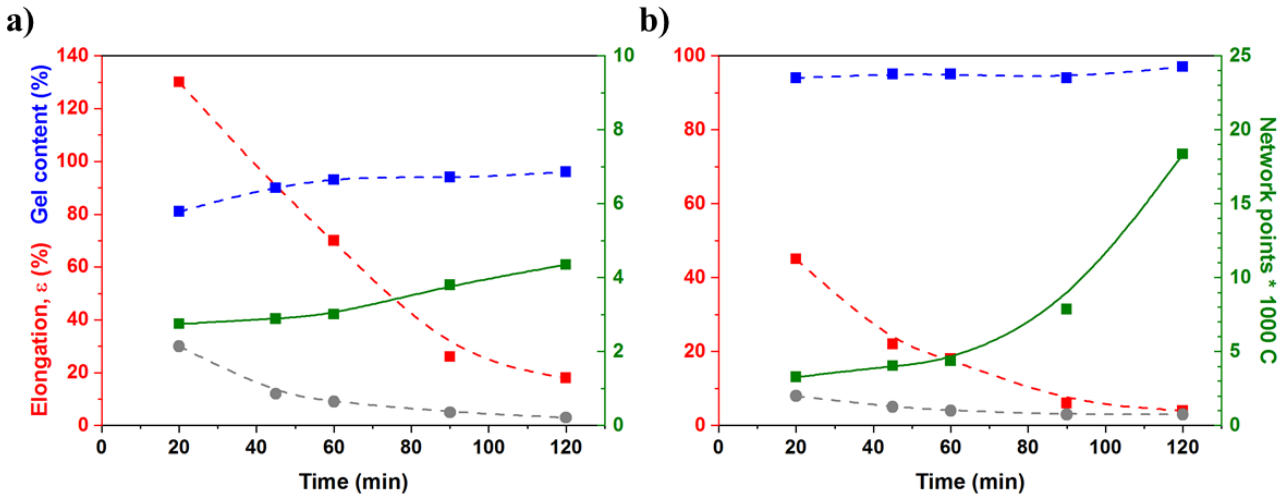

Figure 24: Hot set elongation ε_{hot} (■), gel content (■), network points per 1000 carbons (■) and permanent elongation (●) of p(E-*stat*-GMA$_8$) crosslinked with **a)** 1 wt% EDA and **b)** 2 wt% EDA at 240°C for various times.

I followed the curing process with Fourier transform infrared spectroscopy (FTIR) in order to gain additional insight into the rate of epoxy-ring opening. Two characteristic absorptions by the epoxy ring can be observed at 3050 and 911 cm^{-1}, attributed to the C-H tension of the methylene bridge and to the C-O deformation of the oxirane group, respectively.

Since the first band is located close to a more prominent O-H absorption band, I used the C-O signal to follow the curing reaction. The carbonyl peak at 1750 cm^{-1} was used for normalization, allowing me to calculate the number of remaining epoxy rings, while the number of unreacted N-H groups was extrapolated from the stoichiometry of the reaction (Figure 25).

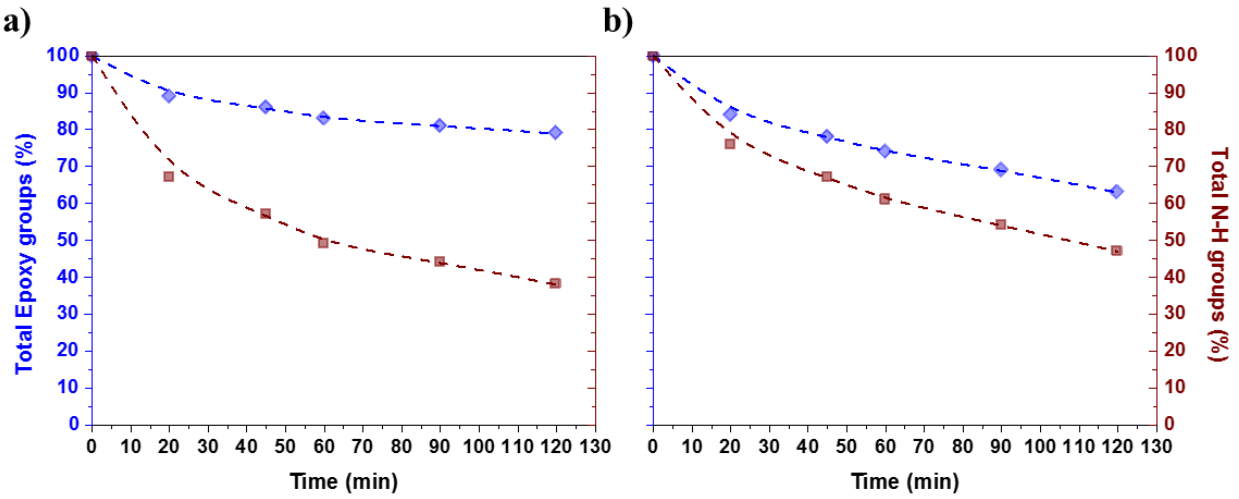

Figure 25: Epoxy (♦) and N-H (■) groups consumption for p(E-stat-GMA_8) crosslinked at 240 °C with **a)** 1 wt% EDA and **b)** 2 wt% EDA, calculated from FTIR.

Consumption of epoxy groups is rapid at first, and starts levelling off after 30 minutes. Even after two hours of curing many N-H functionalities are still left unreacted, which indicates that part of the curing agent has not reacted and may not be part of the crosslinked network. This was confirmed through Thermogravimetric Analysis (TGA). A TGA heating profile that mimics the curing process was selected (two hours at 180 °C), and the results were then compared with standard DCP crosslinking of regular LDPE, using 2 % DCP. p(E-*stat*-GMA_8) samples cured for two hours at 240 °C with 2 wt% EDA and MDA gave rise to a weight loss of 1 and 1.5 %, respectively, which I assign to the release of unreacted curing agent (Figure 26).

Because of the presence of unreacted, volatile curing agents and the overall low reactivity I decided to rule out aromatic diamines as curing agents.

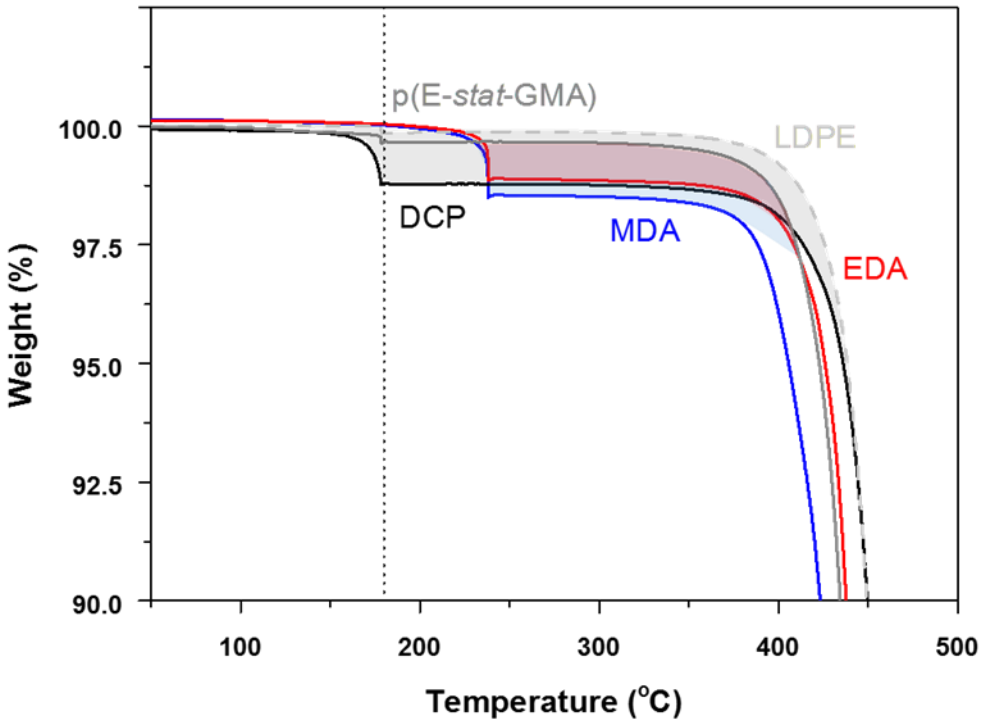

Figure 26: TGA thermograms of neat LDPE, neat p(E-*stat*-GMA$_8$), DCP cured LDPE and p(E-*stat*-GMA$_8$) crosslinked with aromatic amine-based curing agents (MDA, EDA) at 180 °C for 2 hours. The shaded areas highlight the weight loss of volatile by-products that arise from DCP decomposition (grey area) and unreacted aromatic amine crosslinkers (blue and red areas). A baseline drift of not more than 0.4 wt% during the isotherm at 180 °C was recorded.

5.2.2 Aliphatic amine-based curing agents

I chose to study the following aliphatic di- and tri-amines: 1,8-diaminooctane (DAO), N,N'-dimethyl-1,8-octanediamine (MDAO) and trimethylolpropane tris [poly(propylene glycol), amine terminated] ether (TMPTA) (Figure 27). DAO and MDAO carry two primary and secondary amines, respectively, and the melting temperature can be adjusted by changing the length of the aliphatic spacer with an octyl segment resulting in a well-adjusted T_m ~ 40 °C and 50 °C, respectively. TMPTA carries three primary amines and is a liquid at room temperature.

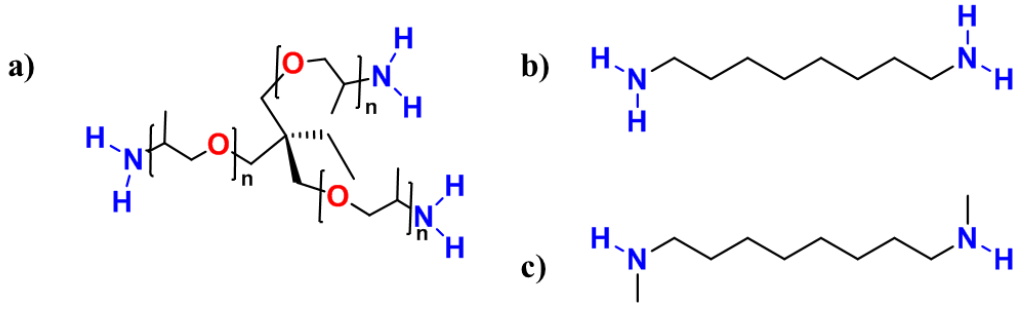

Figure 27: The aliphatic amine-based crosslinkers object of this study: **a)** trimethylolpropane tris [poly(propylene glycol), amine terminated] ether (TMPTA), **b)** 1,8-diaminooctane (DAO), **c)** N,N'-dimethyl-1,8-octanediamine (MDAO).

I proceeded with the study of the reaction conditions with regard to curing time (10 to 120 minutes), temperature (160 to 200 °C) as well as curing agent concentration (c.f. Paper I, Figure 5). Further, I evaluated the crosslinking efficiency by measuring the elongation ε_{hot} and gel content of all samples. I found that all formulations can give rise to a ε_{hot} < 70 % and high gel > 80 % by tuning the aforementioned conditions, which demonstrates the flexibility of these systems (for details, refer to Paper I). The samples did not show any noticeable yellowing usually associated with amine oxidation and retained the typical white color of LDPE.

However, compared to neat p(E-*stat*-GMA_8) the cured samples appeared more transparent. The formation of a dense crosslinking network leads to a less crystalline material, less light scattering and thus increased transparency.

I used TGA to test for volatile by-products (c.f. Paper I, Figure 4c). For neat LDPE and p(E-*stat*-GMA_8), as well as p(E-*stat*-GMA_8) that contained aliphatic amine curing agents I observed a flat TGA thermogram up to 300 °C. No release of by-products could be detected.

Although DAO offers twice as many reactive hydrogens than MDAO, their crosslinking performance is similar for 1 wt% concentration of curing agent. I propose that upon reaction of a primary amine with an oxirane ring, the secondary amine generated from the reaction is more likely to react with a close-by epoxy group from the same polymer chain, due to a combination of steric hindrance and proximity. Therefore, curing agents that carry primary or secondary amines yield a similar number of network points. The lower curing rate of TMPTA formulations can be rationalized with the larger size of this crosslinking agent as well as increased steric hindrance of the amine group due to the adjacent methyl group at the α position. I therefore concluded that the steric hindrance is once again the major contributor.

More information about the curing rate could be obtained through FTIR analysis (c.f. Paper I, Figure 6). Epoxy group consumption is fast at first, followed by a more gradual decrease in reactivity. This is in contrast to a linear increase in network density as calculated from hot set measurements (c.f. Paper I, Figure 5). I propose that, initially, a significant number of curing agents bind with both heads to the same polymer chain, leading to a rapid consumption of epoxides by intra-chain coupling (Figure 28a).

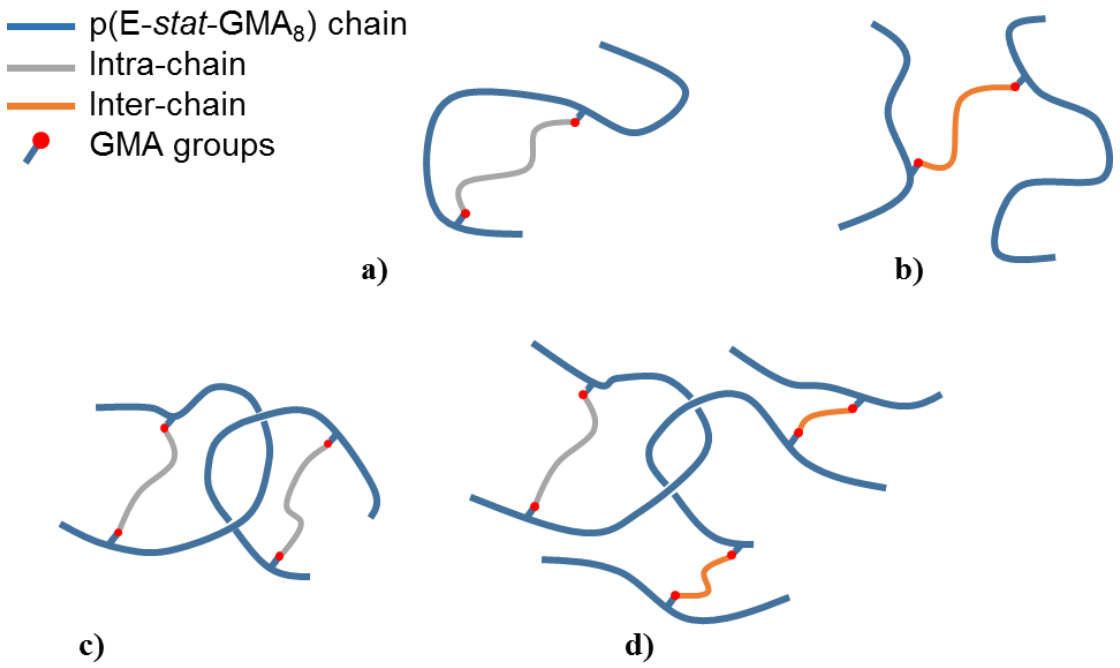

Figure 28: Schematic representation of **a)** an intra-chain crosslink, **b)** an inter-chain crosslink, **c)** a permanent network point that arises due to an entanglement that is trapped by two intra-chain crosslinks, and **d)** an entanglement that is trapped by a combination of intra- and inter-chain crosslinks. Note that this schematic only strictly applies for MDAO where each functional group can only react once with an epoxy ring.

Considering that the used p(E-*stat*-GMA_8) grade contains approximatively 8 glycidyl methacrylate monomers, I note that the number of network points, namely 12 and 10, exceeds the number of oxirane rings (c.f. Paper I, Figure 5). That observation implies the presence of entanglements which are trapped by a combination of spatially close intra- and inter-chain crosslinks (Figure 28c-d).

5.2.2 Hydrazide-based curing agents

Hydrazides are characterized by a N-N covalent bond with four substituents, of which at least one of them is an acyl group. Hydrazides typically present two active hydrogens; thus epoxy resin formulations typically contain ¼ di-hydrazide for each epoxy equivalent. Hence, all four of the primary hydrogens have the possibility to react, each with one epoxy group (Figure 29).

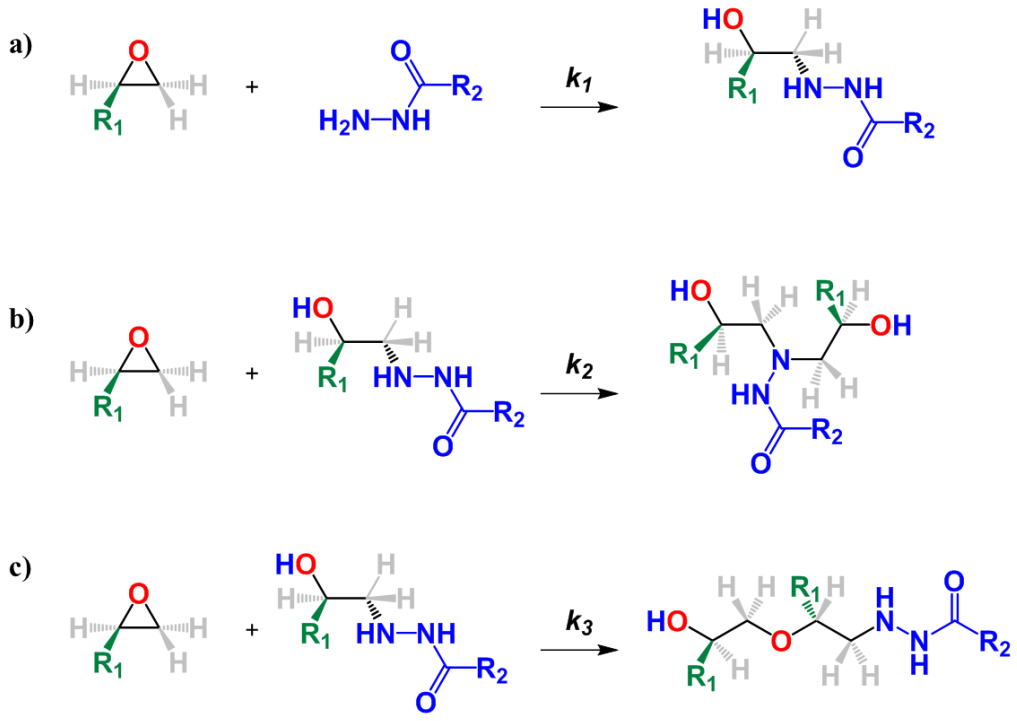

Figure 29: a-b) Epoxy-hydrazide reactions and **c)** epoxy-hydroxy (etherification) side reaction.

Hydrazides tend to have high melting and boiling points, and generally the epoxy-curing temperature is related to the melting temperature of the di-hydrazide. Note that the crosslinking of epoxy resins with dihydrazides can be accelerated with various free-electron-donating compounds, such as ureas, imidazoles and imidazole adducts, as well as inorganic compounds like lead or stannous octoate, which is not explored in this thesis.

Low molecular weight dihydrazides are often toxic. On the other hand, their non-toxic higher molecular-weight counterparts have too high melting points. I therefore selected octanoic hydrazide (OAD) and adipic acid di-hydrazide (AAD), which meet close to all requirements, for initial screening. However, I was unable to reproducibly crosslink the copolymer at 200 °C, even after 2 hours and with a 3 wt% curing agent concentration. I therefore decided to disregard hydrazides as curing agents.

5.2.3 Phenol-based curing agents

The reaction between a phenolic functional group and an epoxy ring is known to be fast, and occurs without the release of any by-product (Figure 30a). Further, the reaction results in the formation of a mixture of isomeric products characterized by a hydroxyl group, which is capable of reacting with other epoxy rings if the reaction proceeds at high temperature and/or in the presence of a catalyst. Epoxy ring-opening by an alcohol also leads to a crosslink and will again generate a hydroxyl group (Figure 30b).

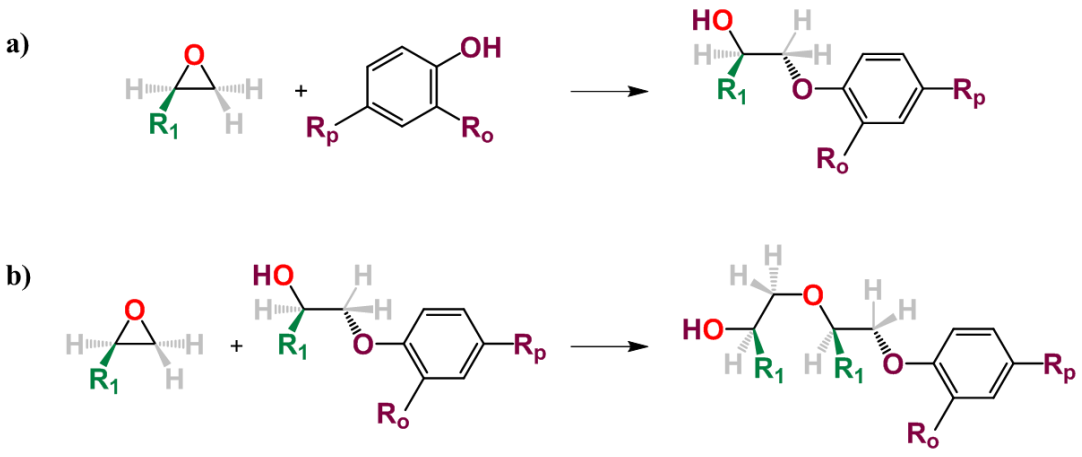

Figure 30: a) Epoxy-phenol reaction and **b)** epoxy-hydroxy side reaction.

I decided to study curing with two different multi-phenols, namely 2,2-bis (4-hydroxy-3-methylphenyl) propane (BPP), and pentaerythritol tetrakis (3-(3,5-di-tert-butyl-4-hydroxyphenyl) propionate) (PTP) (Figure 31).

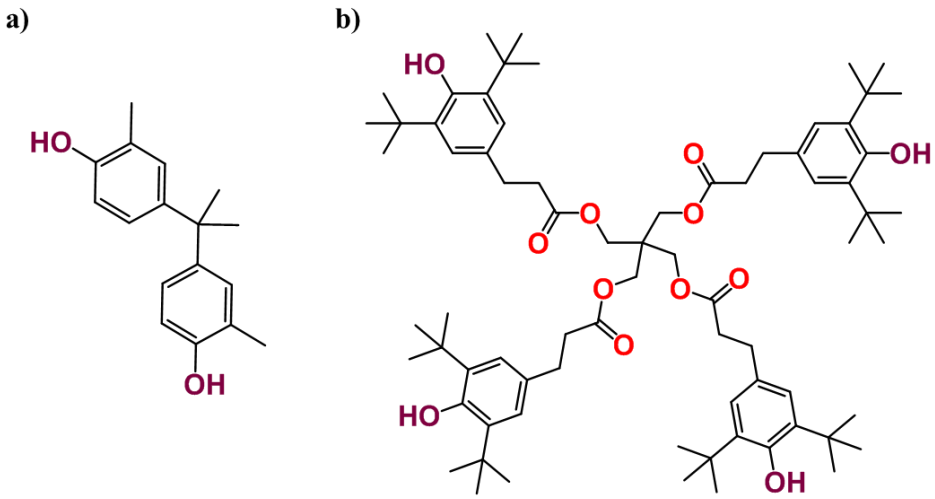

Figure 31: The phenol-based crosslinkers object of this study: **a)** 2,2-bis (4-hydroxy-3-methylphenyl) propane (BPP), **b)** Pentaerythritol tetrakis (3-(3,5-di-tert-butyl-4-hydroxyphenyl) propionate) (PTP).

BPP is a non-toxic, low molecular weight chemical, with a boiling point above the curing temperature; it has two phenolic functionalities, making it a multifunctional hardener. PTP is a non-toxic, high molecular-weight chemical that finds use as an antioxidant. PTP bears four phenolic functionalities, and it is much bulkier and sterically hindered compared to BPP, in particular thanks to its tert-butyl groups in ortho-position. At first, I evaluated the crosslinking efficiency of BPP by measuring the elongation ε_{hot} of p(E-*stat*-GMA$_8$) samples cured at different temperatures (between 160 and 240 °C) and with 3 wt% BPP, which corresponds to a stoichiometric ratio of 2.3:1 epoxy:phenol functionalities.

The aforementioned formulation was cured at various times, ranging from 5 to 120 minutes (Figure 32a-b). I concluded that sufficient crosslinking could be achieved by curing the resin for at least 20 minutes at 240 °C.

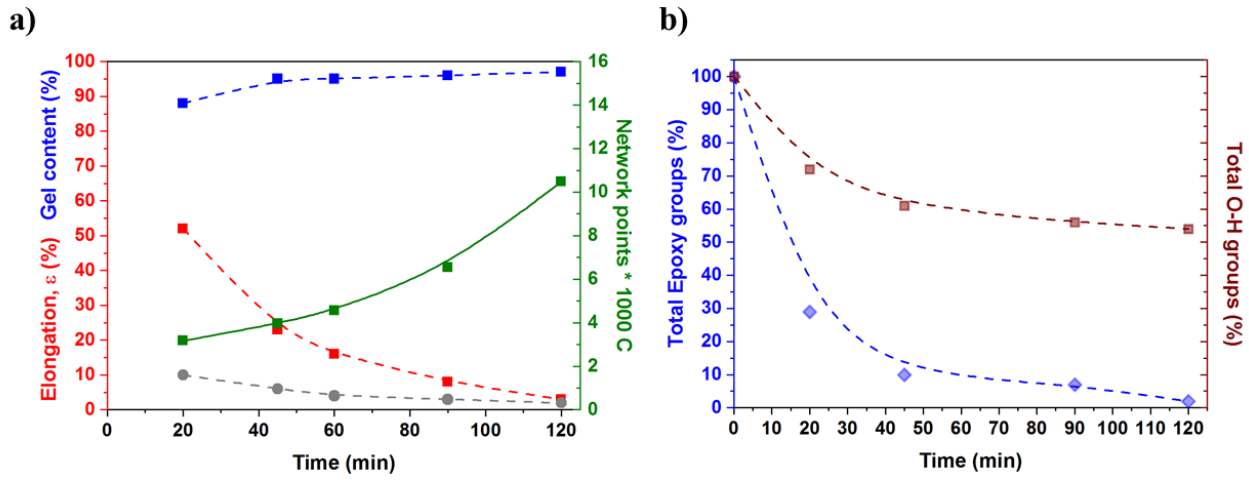

Figure 32: a) Hot set elongation ε_{hot} (■), gel content (■), network points per 1000 carbons (■) and permanent elongation (●) of p(E-*stat*-GMA$_8$) crosslinked with BPP 3% at 240°C for various times, **b)** consumption of epoxy (♦) and phenolic (■) groups from FTIR.

The crosslinking efficiency of PTP:p(E-*stat*-GMA$_8$) with a 4 or 8 wt% curing agent content (which corresponds to a stoichiometric ratio of 4:1 and 2:1 epoxy:phenol functionalities, respectively) was tested at different temperatures (160 to 280 °C) (Figure 33a-b).

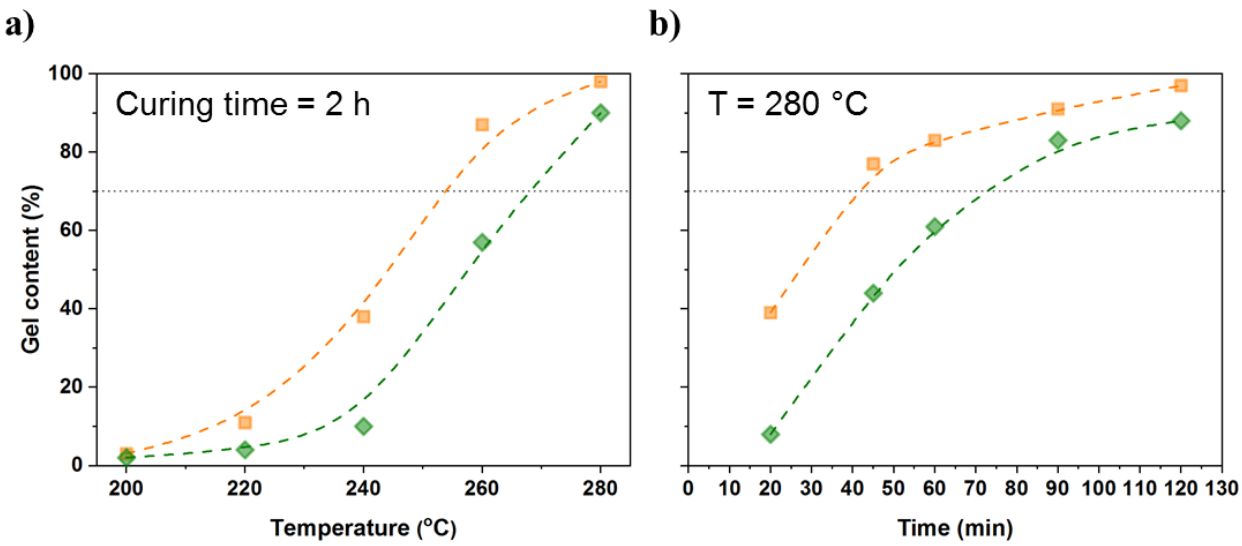

Figure 33: Gel content measurements for p(E-*stat*-GMA$_8$) resin cured with 4 (♦) and 8 wt% (■) PTP at **a)** different temperatures for 2 hours and **b)** different times at 280 °C.

I concluded that curing with PTP is too slow and requires a relatively high temperature, most likely due to its size and steric hindrance. Therefore, I decided to focus on BPP instead.

5.2.4 Lewis acid assisted crosslinking of p(E-*stat*-GMA$_8$) formulations

Despite successful crosslinking at relatively low temperatures with both aliphatic amine and phenol-based curing agents, it was evident that the curing reactions were too slow to be of practical interest. During cable production the length of the curing oven allows for a crosslinking time of typically less than five minutes, after which the insulation layer must be fully cured (c.f. Figure 3). Therefore, I concluded that a catalyst is required to speed up the crosslinking process. I tested several Lewis acids, and after an initial screening I concluded that titanate-based compounds provided the best results. In particular, titanium (IV) 2-ethylhexyloxide (Ti(2-EtHexO)$_4$; c.f. Paper II, Figure 1) was selected for more extensive studies. Ti(2-EtHexO)$_4$ is moisture and oxygen

resistant, has a high boiling point (~ 250 °C), is liquid at room temperature, non-toxic, relatively inexpensive and easy to handle.

The catalyst was incorporated in different p(E-*stat*-GMA_8) formulations, in combination with the already studied aliphatic amines DAO and TMPTA, and the phenol-based curing agent BPP. I found that the incorporation of as little as 0.5 wt% of $Ti(2\text{-}EtHexO)_4$, which corresponds to merely 0.04 wt% elemental titanium, greatly reduced the time necessary to achieve a high degree of crosslinking. The compounding of the Lewis acid, the crosslinking agent and the copolymer through extrusion at 120-140 °C can be carried out without onset of the curing reaction. Then, at more elevated temperatures of 180 °C and above, rapid crosslinking occurs at a much faster rate as compared to non-catalyzed formulations.

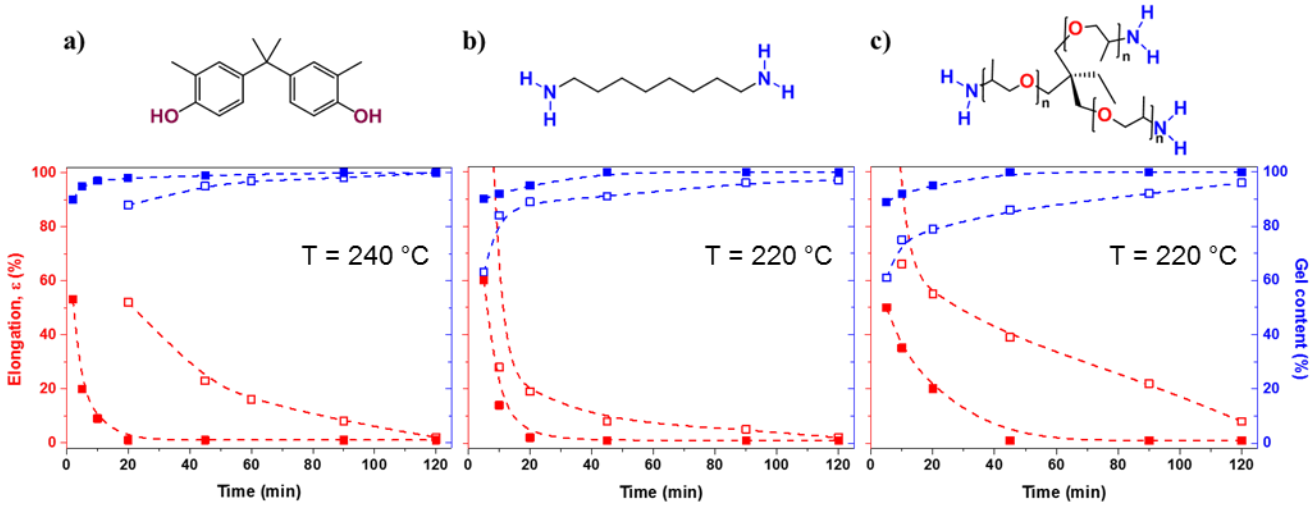

Figure 34: Hot set elongation (red) and gel content (blue) of p(E-*stat*-GMA_8) crosslinked with **a)** BPP 3 wt% (hollow squares) and BPP 3 wt% + 0.5% Ti (full squares) at 240 °C for 2.5 to 120 minutes, **b)** DAO 1 wt% (hollow squares) and DAO 1 wt% + 0.5% Ti (full squares) at 220 °C for 5 to 120 minutes, and **c)** TMPTA 2 wt% (hollow squares) and TMPTA 2 wt% + 0.5% Ti (full squares) at 220 °C for 5 to 120 minutes.

I measured the gel content and elongation at break of three types of formulations: p(E-*stat*-GMA_8) cured with (1) 1 wt% DAO, (2) 2 wt% TMPTA, and (3) 3 wt% BPP. In each case I compared crosslinking of the neat formulations with the $Ti(2\text{-}EtHexO)_4$ catalyzed ones (0.5 % catalyst added). Amine-based formulations were cured at 220 °C, while the phenol-based one was cured at 240 °C due to its slower reaction rate (Figure 34). All formulations can be cured in under five minutes. The impact of the catalyst on crosslinking with BPP was particularly dramatic (c.f. Paper II), which I attributed to in-situ generation of a new titanium-phenoxide catalyst. I observed a bright orange color, which I proposed to originate from a ligand-exchange between alcohol and phenol groups on the titanium atom, and hence the formation of a new species bearing phenoxide ligands. I found that adding as little as 0.5 wt% of $Ti(2\text{-}EtHexO)_4$ to a p(E-*stat*-GMA_8) resin containing 3 wt% BPP gave rise to a hot set elongation as low as ε_{hot} < 50 % for a crosslinking time of only 2 minutes at 240 °C (cf. Paper II, Figure 3). To gain deeper understanding of the behavior and efficiency of the crosslinking reaction, I performed a series of experiments for a fixed time of 5 minutes and I found that the temperature strongly affects the hot set elongation.

Phenols easily react with alkoxides releasing alcohols and leading to the formation of the corresponding phenoxide. I propose that a ligand-exchange between alcohol and phenol groups on titanium occurs leading to the formation of a new species bearing phenoxide ligands (Figure 35a). Those result in numerous possible reactive species, all of which can contribute to epoxy ring-opening reactions and consequently to the curing of p(E-*stat*-GMA_8). In case of the non-catalyzed reaction, an epoxy ring-opening reaction would be initiated by the phenol attacking the less hindered carbon atom of the oxirane ring, generating an alcohol. The generated alcohol is usually not reactive enough to attack another epoxy ring without the presence of a catalyst, and the polyaddition cannot proceed further. Therefore, to generate a network point the second phenol functionality that the hardener is bearing must react as well, creating a bridge between two different

polymer chains. In the case of a titanium phenoxide catalyst generated in-situ, however, the attack on an epoxy ring would lead to the formation of a titanium alkoxide group (Figure 35b), which subsequently would be reactive enough to interact with the next epoxy ring, propagating an epoxy-epoxy poly-addition (Figure 35c). Moreover, the generated titanium alkoxide can also undergo a ligand exchange with another 2,2-bis(4-hydroxy-3-methylphenyl)propane molecule and regenerate the catalytic species (Figure 35d).

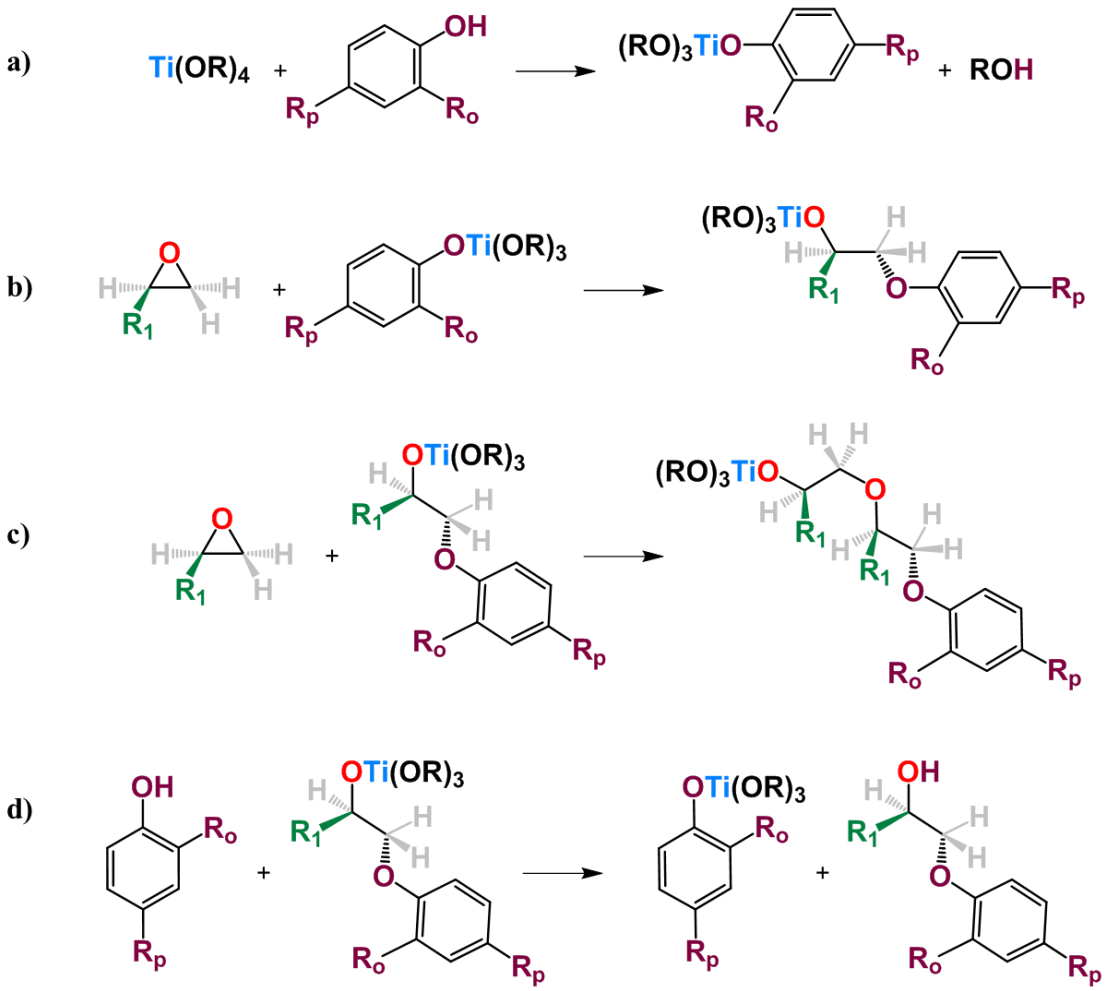

Figure 35: Lewis-acid catalyzed phenol-epoxy ring-opening reactions: **a)** phenol deprotonation and generation of a phenolate, **b)** epoxy-phenolate reaction and generation of a hydroxylate, **c)** epoxy-hydroxylate reaction (epoxy homopolymerization), **d)** regeneration of phenolate.

Solid-state ^{13}C NMR was performed on a cured p(E-*stat*-GMA_8):BPP:Ti specimen after solvent extraction, and the result showed a significant intensity reduction for the carbon signals corresponding to the three carbons in and near the epoxy ring after curing, as well as a slight downfield change in their chemical shift (Figure 36).

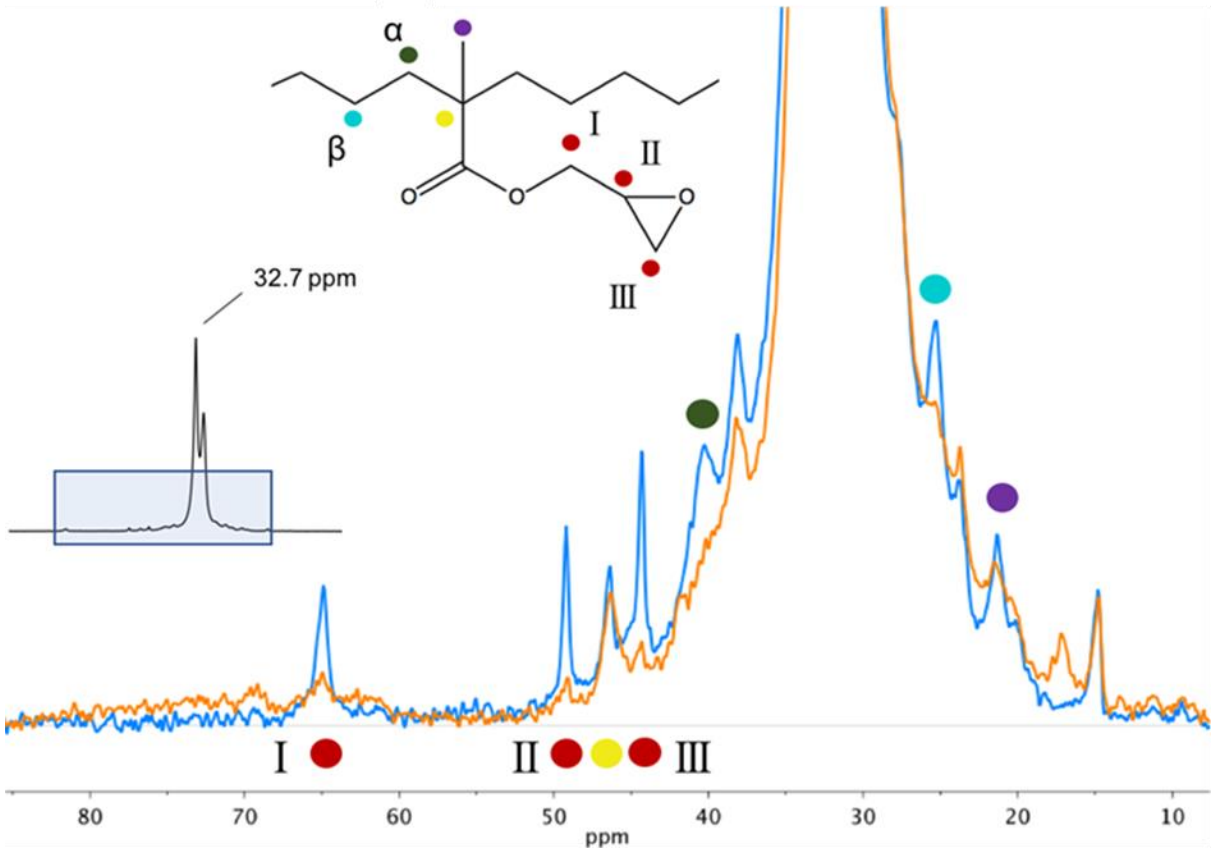

Figure 36: Magnified part of the solid-state ^{13}C CP/MAS NMR spectra of p(E-*stat*-GMA_8) (blue) and p(E-*stat*-GMA_8) cured with 6% BPP and 0.5% $Ti(2\text{-}EtHexO)_4$ (orange). Color-coded circles refer to the carbons in the molecular structure of p(E-*stat*-GMA_8); the entire spectrum is shown as an insert to the left. *Reproduced with permission from the Royal Society of Chemistry (RSC).*

Moreover, the sharp and well isolated peak at 17.2 ppm, attributed to the two methyl groups that sit in ortho-position on the aromatic rings of BPP, reveals the presence of the curing agent. This observation is therefore evidence for the participation of phenol-epoxy ring opening reactions in the curing of the polyethylene copolymer. I concluded that the exceptional performance of formulations containing an amine or phenol curing agent and a Lewis acids catalyst are a viable, industrially and economically interesting, by-product free alternative to peroxide-based crosslinking of polyethylenes.

CHAPTER 6

6.1 Crosslinking of polyethylene copolymers blends

Since the use of low molecular weight crosslinking agents can result in a fraction of unreacted additive I explored an alternative approach based on blending of two polyethylene-based copolymers. The judiciously chosen functionalities will be able to react in a click chemistry fashion upon heating. Every reaction between comonomers will generate at least one network point, with the possibility of generating more in case of trapped entanglements (c.f. Figure 37).

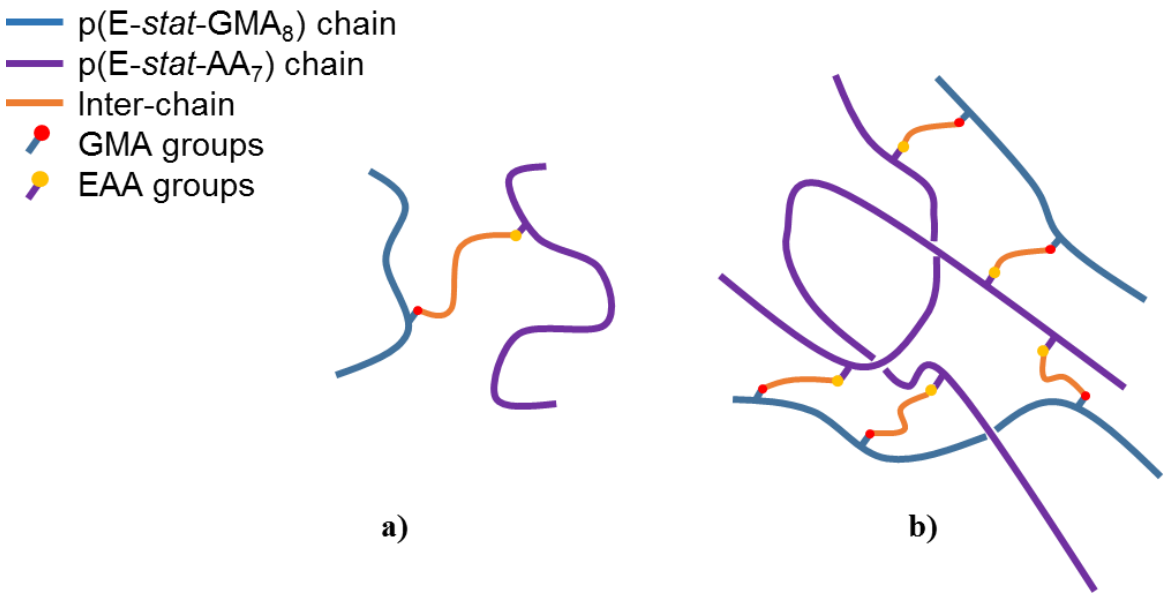

Figure 37: Schematic representation of **a)** an inter-chain crosslink, **b)** an entanglement that is trapped by several inter-chain crosslinks.

It is essential that such copolymer blends can be extruded between 120 and 140 °C whilst avoiding the curing reaction. In a second step, upon raising the temperature to more than 160 °C, rapid curing should occur.

6.2 Crosslinking of binary p(E-*stat*-GMA$_8$):p(E-*stat*-AA$_7$) blends

I decided to explore a blend that consists of the already introduced statistical ethylene-glycidyl methacrylate copolymer, p(E-*stat*-GMA$_8$), and a statistical ethylene-acrylic acid copolymer with a comonomer content of 7 wt%, p(E-*stat*-AA$_7$) (Figure 38).

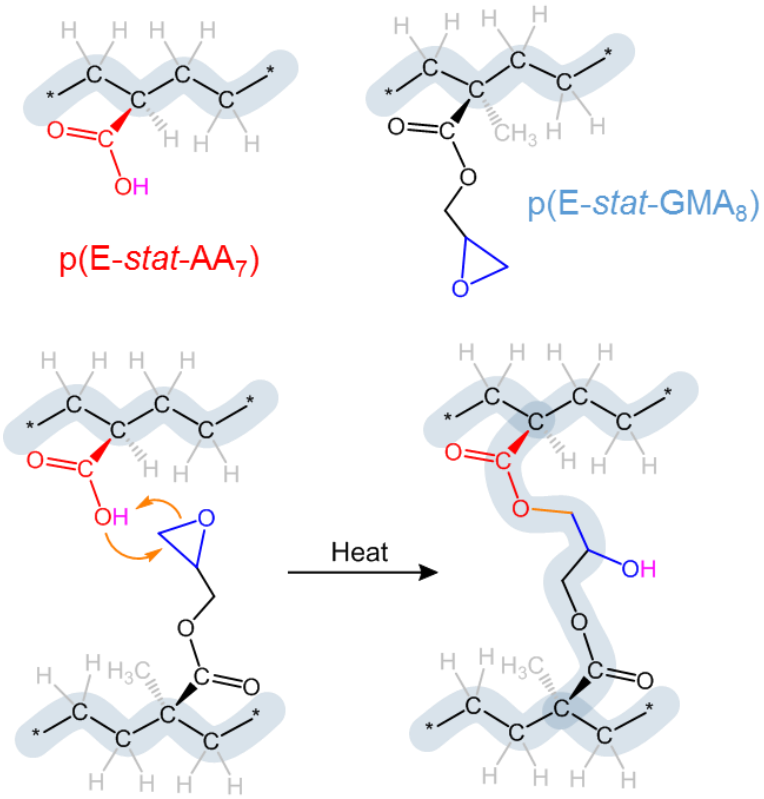

Figure 38: The branched statistical ethylene-acrylic acid p(E-*stat*-AA$_7$) and ethylene-glycidyl methacrylate copolymer p(E-*stat*-GMA$_8$) used in this study, with a comonomer content of 7 and 8 wt%, respectively. At the bottom, the reaction scheme for p(E-*stat*-AA$_7$) with p(E-*stat*-GMA$_8$). *Reproduced with permission from the Royal Society of Chemistry (RSC).*

The uncatalyzed reaction between epoxy and carboxyl groups will yield (1) the ester of the primary hydroxyl group, which will covalently link the two polymers, and (2) a hydroxyl group that arises due to opening of the epoxy ring (Figure 39a).[93, 94]

Excess of either comonomer may result in a follow-up reaction involving the latter, provided that the temperature is sufficiently high. An excess of glycidyl methacrylate may react with the hydroxyl group resulting in ether formation but no by-products (Figure 39b). On the other hand, excess carboxylic acid may react with the hydroxyl group leading to complete esterification and the release of water as a by-product (Figure 39c). The released water can also react with epoxy rings, generating a diol (Figure 39d).

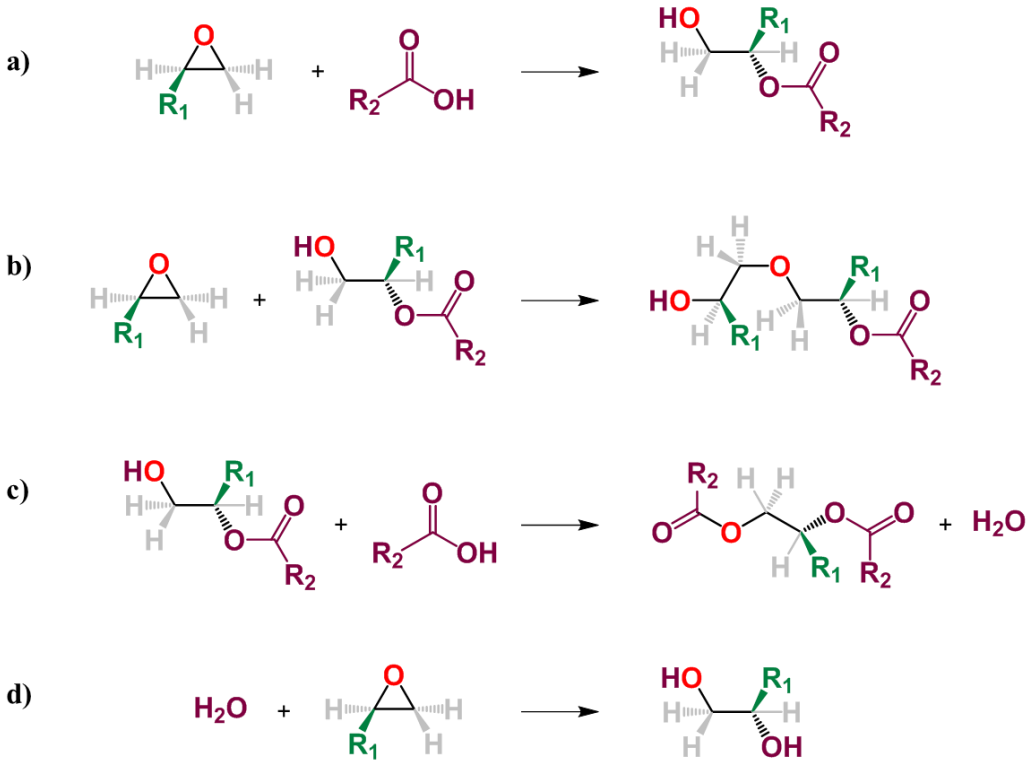

Figure 39: a) Epoxy-carboxylic acid reaction, **b)** epoxy-hydroxy reaction, **c)** esterification reaction, and **d)** epoxy ring-opening reaction in the presence of water.

It would be possible to avoid complete esterification and water release by adding a base as a catalyst to the resin, but I did not decide to opt for this solution in order to maintain an additive free formulation. Instead, I chose to work with a 1.7:1 p(E-*stat*-GMA_8):p(E-*stat*-AA_7) blend

stoichiometry, so that an equal amount of each comonomer is present. FTIR analysis on a series of films crosslinked at 200 °C for different amounts of time was carried out in order to investigate if any side reaction takes place during crosslinking (c.f. Paper III). I could observe that the epoxy and carboxylic acid are consumed at the same rate, which suggests that the two groups react with each other and that the above-mentioned side reactions are largely absent (c.f. Paper III, Figure S1). Further, I ruled out esterification because of the absence of the prominent water absorption band in the region between 3500-3700 cm^{-1}, associated with symmetric and asymmetric stretching of O-H groups. TGA was also performed in order to strengthen the claim that no by-product is generated by the curing reaction.

The thermoplastic copolymer blend offers a broad processing window up to 140 °C, where compounding and shaping can be carried out without curing. At more elevated temperature epoxy and acrylic acid functionalities rapidly react to form an infusible network. I compounded the two copolymers by co-extrusion at 120 °C (see Paper III for details) and obtained a visually homogeneous extrudate. It can be anticipated that a certain degree of miscibility is required to facilitate proximity of the glycidyl methacrylate and acrylic acid comonomers throughout the blend, which is a prerequisite for them to undergo a crosslinking reaction. FTIR spectra of p(E-*stat*-AA_7) collected while increasing the temperature showed that the acid groups are predominantly present in the dimerized state up to at least 90 °C.[98] Instead, the relative amount of acid dimers strongly decreased upon blending: since acid dimers reside only in the amorphous phase,[99, 100] this indicates at least partial miscibility of the two copolymers in the amorphous phase (Figure 40).

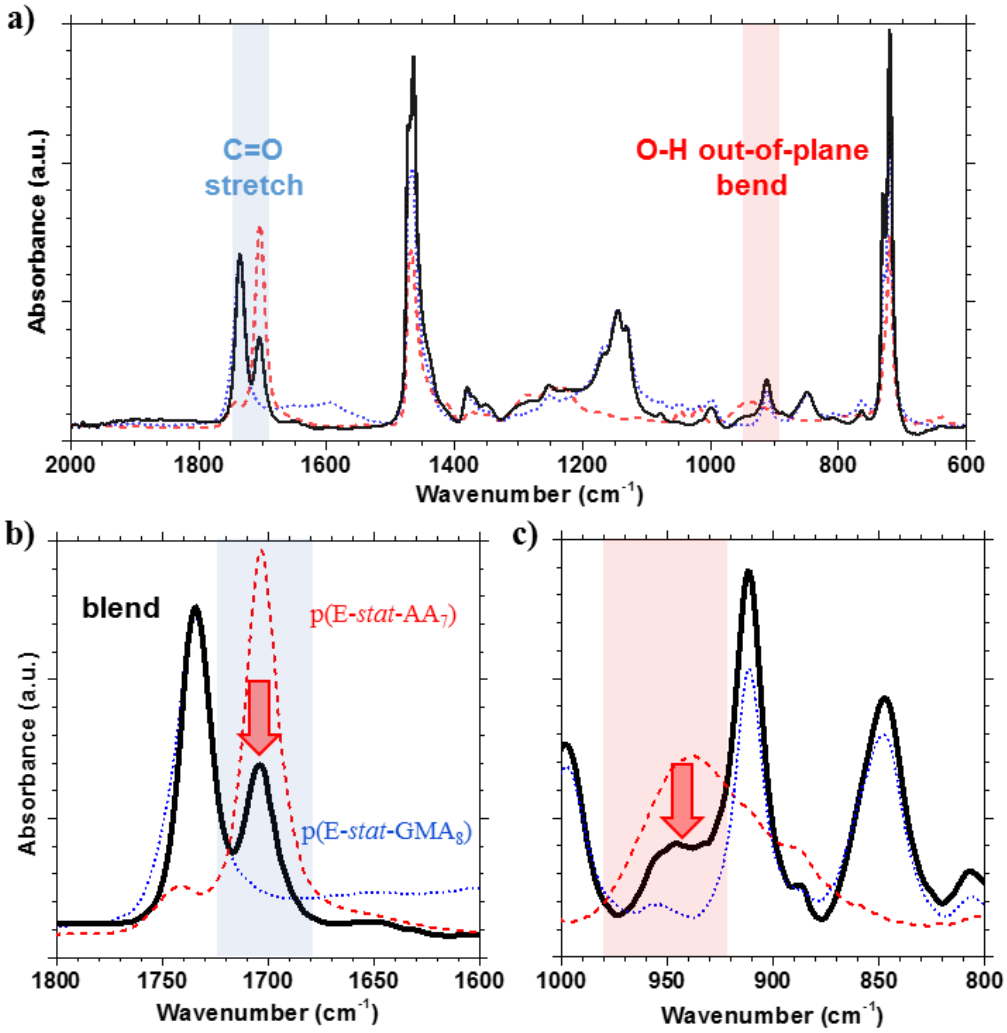

Figure 40: a) ATR-FTIR spectrum of p(E-*stat*-GMA_8):p(E-*stat*-AA_7) polymer blend at stochiometric ratios. **b)** C=O stretch region, peak at 1705 cm^{-1} significantly reduced, **c)** O-H out of plane bend, peak at 940 cm^{-1} significantly reduced. All spectra are normalized and p(E-*stat*-AA_7) and p(E-*stat*-GMA_8) intensities are scaled to their respective blend concentration. Blend (**solid**); p(E-*stat*-GMA_8) (dashed); p(E-*stat*-AA_7) (dotted). *Reproduced with permission from the Royal Society of Chemistry (RSC).*

Thermal analysis was used to confirm that the here studied copolymer blend is miscible, using co-crystallization as an indicator. The presence of a single broad melting endotherm when reheating extruded material is evidence for co-crystallization in melt-miscible polyethylene blends. Instead, material that was cooled more slowly, i.e. at 10 °C min^{-1}, featured two distinct melting endotherms. I went on to study the rate of crosslinking of the 1.7:1 p(E-*stat*-GMA_8):p(E-*stat*-AA_7) blend at different temperatures between 160 and 200 °C (for details, see Paper III). Further, I studied network formation as a function of time at a fixed temperature of 200 °C (Figure 41a-e). I used two techniques to calculate the number of network points, (1) hot set elongation measurements and (2) DMA according to the methods reported in Paper III (c.f. equations 2 and 3, respectively). Already after a curing time of 2.5 minutes at 200 °C I calculated a network density comparable with the one achieved with DCP crosslinking under the same conditions suggesting that the here studied copolymer blend rapidly reacts to form an infusible network. In the crosslinked blend two types of network points exist in the molten state, (1) covalent crosslinks due to the reaction between the glycidyl methacrylate and acrylic acid comonomers, and (2) trapped entanglements (Figure 41e). I followed the epoxy ring consumption with FTIR in order to elucidate the extent to which each type contributes to the overall number of network points. Each epoxy ring opening reaction gives rise to *one* covalent crosslink. Comparison between the number of covalent crosslinks (from FTIR) and the total number of network points (from DMA and hot set elongation) indicates that trapped entanglements become more prominent as soon as more than half the epoxy rings are consumed (Figure 41c).

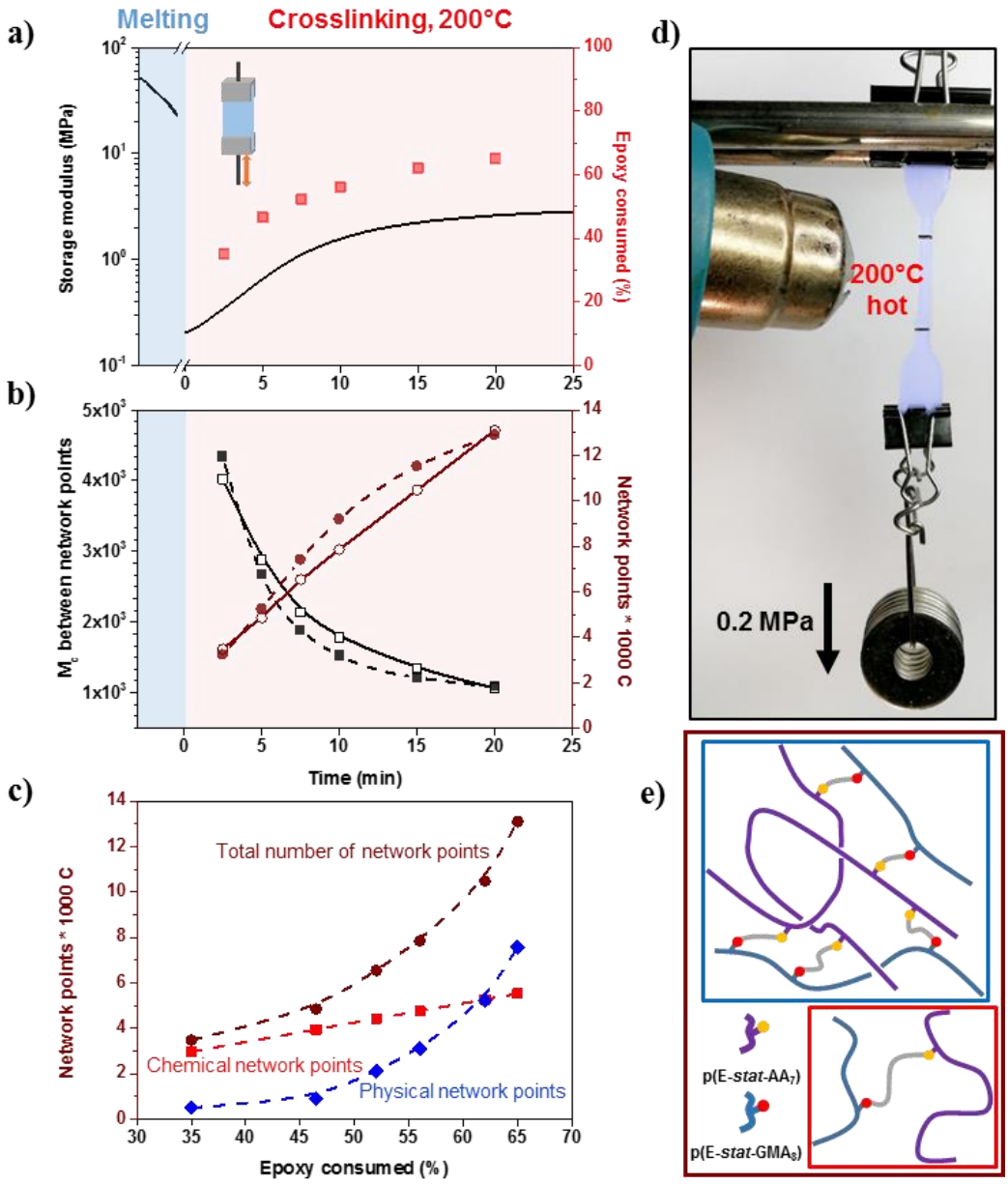

Figure 41: a) Storage modulus evolution with time at 200 °C in DMA and relative epoxy consumption (□), **a)** Network point formation per 1000 carbons (● calculated from hot set, ○ from DMA) and relative molecular weight between crosslinks, M_c (■ calculated from hot set, □ from DMA), **c)** Network point composition (■ chemical, ♦ physical and ● total) for a 1:1 stoichiometric p(E-*stat*-GMA_8):p(E-*stat*-AA_7) formulation cross-linked at 200 °C, **d)** heating of a dogbone of p(E-*stat*-GMA_8):p(E-*stat*-AA_7) crosslinked for 5min at 200 °C (false-colored in blue), and **e)** illustration of a trapped entanglement (blue box) and a chemical crosslink (red box). *Reproduced with permission from the Royal Society of Chemistry (RSC).*

To determine the DC electrical conductivity, a series of broadband dielectric spectroscopy (BDS) measurements was carried out. The conductivity measured with BDS shows a marked frequency dependence, in particular at high frequencies. However, at sufficiently low frequencies the conductivity is only determined by the migration of charge carriers and approaches a constant value. This plateau was used to estimate σ_{DC}. LDPE yielded a value of $\sigma_{DC} \sim 1.8 \cdot 10^{-16}$ S cm^{-1} at 70 °C, which is in good agreement with a previous report, although measured at lower fields.[11] At a temperature of 70 °C the thermoplastic and crosslinked copolymer blend gave σ_{DC} values of ~ $1.3 \cdot 10^{-16}$ S cm^{-1} and $2 \cdot 10^{-16}$ S cm^{-1} respectively. It appears that despite the presence of polar comonomers the conductivity of the here studied copolymer blend is not negatively affected. Both, the thermoplastic and crosslinked copolymer blend display a very low DC electrical conductivity on the order of 10^{-16} S cm^{-1}, a value which is at par with values measured for both ultra-clean LDPE as well as a commercial XLPE grade. A more in depth discussion about conductivity measurements can be found in Paper III. I concluded that the here explored by-product free crosslinking concept opens up the possibility to replace peroxide crosslinking with click chemistry type reactions.

6.3 Crosslinking of ternary p(E-*stat*-GMA$_8$):p(E-*stat*-AA$_7$):LDPE blends

To be a real breakthrough in the field of power cable insulation and in order to be economically and technically appealing at an industrial level, pre-crosslinking behavior of p(E-*stat*-GMA$_8$) formulations over an extended period of time must be minimized. Despite being much slower, gradual curing of p(E-*stat*-GMA$_8$) and p(E-*stat*-AA$_7$) occurs also at extrusion temperatures, around 120-140 °C (c.f. Paper III). This is not a problem for short dwell times, but it may generate an infusible network when the material stagnates in an extruder. I therefore went on to study if pre-crosslinking can be reduced by altering the amount of available functional groups. I chose two approaches: (1) the addition of 50 wt% LDPE to the copolymer blend, thus creating a ternary blend, and (2) a blend of two copolymers that contain a lower content of glycidyl methacrylate and acrylic acid comonomer of 4.5 wt% and 3 wt%, respectively. Initially, I evaluated the performance of 1.7:1 p(E-*stat*-GMA$_8$):p(E-*stat*-AA$_7$) blends containing different amount of pure LDPE, ranging from 10 to 50 wt%, thus reducing the overall comonomer content. I compounded the polymers by co-extrusion at 120 °C and obtained homogeneous extrudates (Figure 42a). These formulations were subsequently crosslinked for 10 minutes at 200 °C, and the crosslinking efficiency was evaluated by comparing the hot set elongation ε_{hot} at 200 °C and a stress of 0.2 MPa. The network density was then calculated based on the molecular weight between crosslinks M_c according to the affine network model,[101] which is applicable to elastomers.

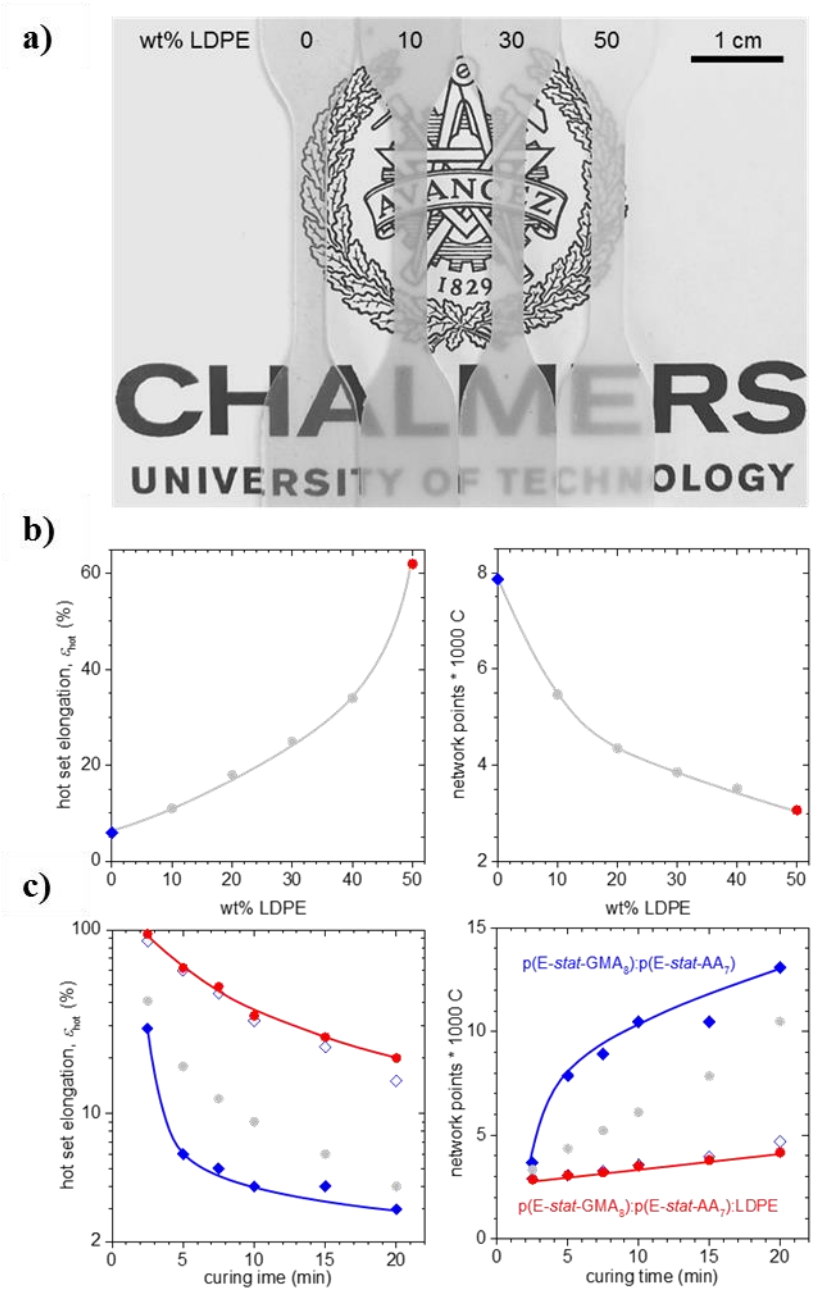

Figure 42: **a)** Photograph of melt pressed dog bones prior to hot set elongation experiments; **b**) hot set elongation ε_{hot} (left) and number of network points per 1000 carbons (right) of binary (♦) and ternary blends (● and ●) cured for 5 minutes at 200 °C; **c**) ε_{hot} (left) and number of network points per 1000 carbons after curing for different times at 200 °C (right) of p(E-*stat*-GMA$_8$):p(E-*stat*-AA$_7$) (♦), p(E-*stat*-GMA$_{4.5}$):p(E-*stat*-AA$_3$) (◊), and p(E-*stat*-GMA$_8$):p(E-*stat*-AA$_7$):LDPE ternary blends containing 30 wt% LDPE (●), and 50 wt% LDPE (●); solid lines are a guide to the eye.

As expected, adding up to 50 wt% LDPE to a stoichiometric p(E-*stat*-GMA_8):p(E-*stat*-AA_7) blend impacts its mechanical properties, increasing ε_{hot} from 6 to 62 % and reducing the number of network points (Figure 42b). Encouraged by these preliminary data I decided to study the network formation as a function of time at a fixed temperature of 200 °C (Figure 42c). I found that 5 minutes curing at 200 °C is enough for all formulations to achieve a sufficiently low ε_{hot}. It is interesting to note that the crosslinking behavior of p(E-*stat*-GMA_8):p(E-*stat*-AA_7) with 50% LDPE and p(E-*stat*-$GMA_{4.5}$):p(E-*stat*-AA_3) blends, which contain a comparable overall comonomer content, is very similar.

Differential scanning calorimetry (DSC) heating thermograms of high LDPE content blends were recorded to gain additional insight into their phase behavior. For the ternary blends I observed two melting peaks in DSC first heating thermograms of as-extruded material (cf. Paper IV). The melting peak at 100 °C corresponds to co-crystals of the two copolymers (note that the neat copolymers melt at 105 °C and 98 °C), whereas LDPE gives rise to a separate peak at 110 °C (note that neat LDPE has a T_m ~ 110 °C). I therefore concluded that the molten ternary blends are phase-separated into domains of p(E-*stat*-GMA_8):p(E-*stat*-AA_7) and LDPE, respectively. This conclusion is supported by atomic force microscopy (AFM) images of ternary blends (Figure 43).

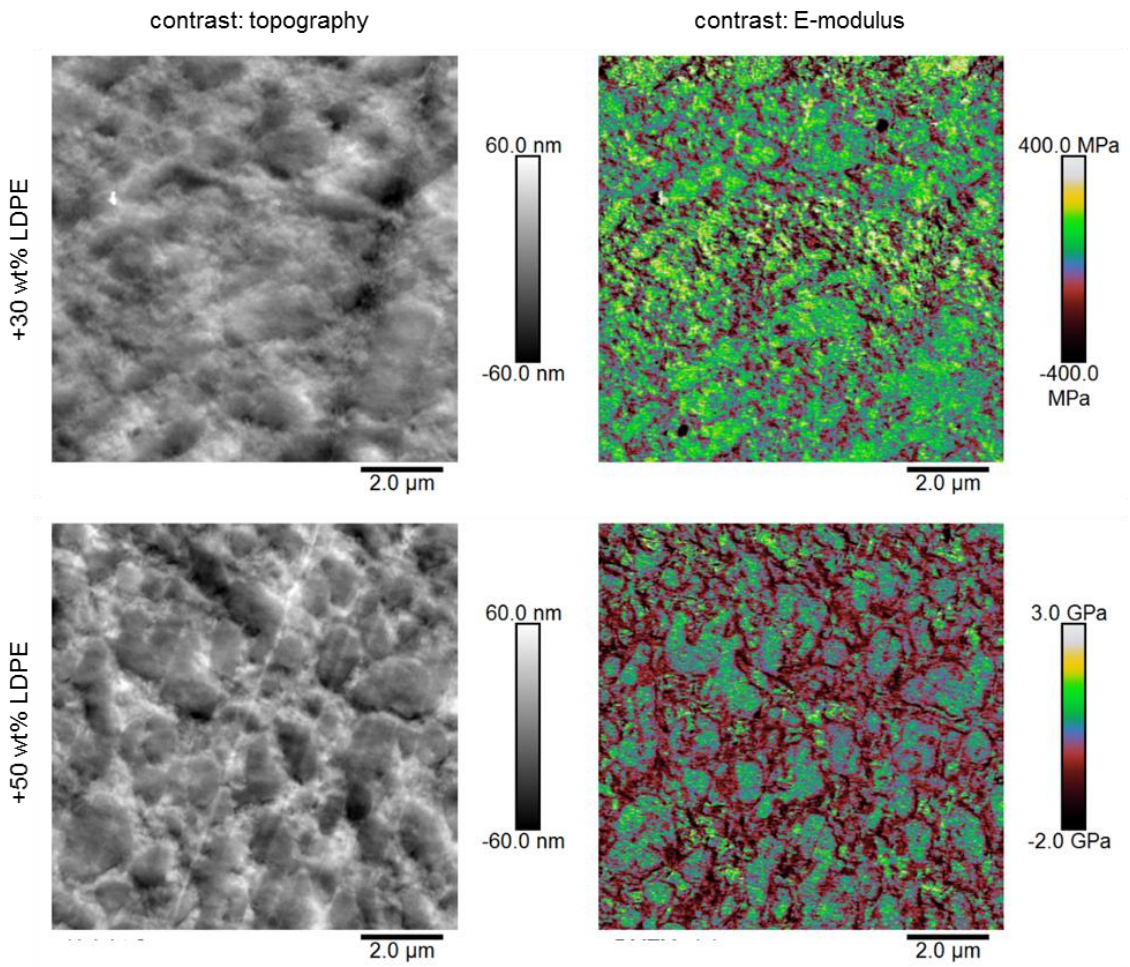

Figure 43: Atomic force microscopy (AFM) images of cryotomed cross sections of ternary blends comprising 30 wt% (top) and 50 wt% LDPE (bottom), recorded in topography mode (left) and E-modulus mode (right); note that the E-modulus scale was not calibrated and should only be used for relative comparison.

To establish the extent to which blending with LDPE allows to increase the extrusion window, I compared the number of network points that form after curing for 5 minutes at different temperatures ranging from 120 to 210 °C (Figure 44). At low temperatures where no appreciable crosslinking occurs and the samples remain thermoplastic, which prevents hot set elongation measurements, I monitored the increase in storage modulus G' with rheometry, and estimated M_c

according to the method reported in Paper IV (c.f. equation 2). At higher temperatures, instead, I used hot set elongation measurements to calculate M_c according to the affine network model (c.f. Paper IV, equation 1). Note that I did not use the plateau modulus to calculate M_c, which should be measured at the frequency where the loss modulus G'' or the loss tangent show a minimum, but instead I used G' measured at a fixed frequency during dynamic curing experiments.[102] Hence, the values obtained for M_c, and the number of network points, should only be used for a semi-quantitative comparison (c.f. Paper IV).

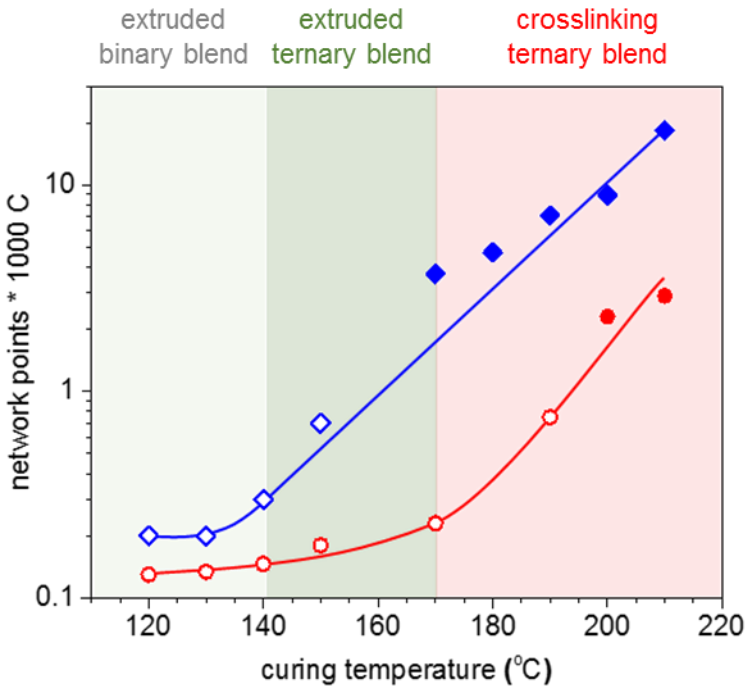

Figure 44: Number of network points per 1000 carbons for p(E-*stat*-GMA$_8$):p(E-*stat*-AA$_7$) binary blends (blue) and p(E-*stat*-GMA$_8$):p(E-*stat*-AA$_7$):LDPE ternary blends containing 50 wt% LDPE (red), determined after 5 minutes of crosslinking with rheometry (open symbols) and hot set elongation measurements (solid symbols); solid lines are a guide to the eye.

I found that across the full studied temperature range the ternary blends cure considerably more slowly. I chose a network density of about 0.3 network points per 1000 carbons as a cut-off, which for the p(E-*stat*-GMA$_8$):p(E-*stat*-AA$_7$) blend corresponds to a gel content of ~ 5 %. I concluded that whereas the binary blend should be extruded below 140 °C to avoid premature crosslinking, the ternary blend containing 50 wt% LDPE can experience temperatures of up to 170 °C without losing its thermoplasticity. In order to assess the long-term effect of premature crosslinking on the rheological properties of ternary blends, I performed dynamic curing experiments at an angular frequency of ω = 1 Hz. I compared the binary blend of p(E-*stat*-GMA$_8$):p(E-*stat*-AA$_7$) with the corresponding ternary blend containing 50 wt% LDPE, and monitored G' and G'' over a period of 15 to 60 minutes at 130 and 150 °C (Figure 45). Moreover, we used G' to calculate the number of network points. I found that the storage modulus of the binary blend increases rapidly, indicating that the curing reaction proceeds, which forced me to terminate the experiments prematurely in order to not fully crosslink the material in the rheometer. Instead, the rheological properties of the ternary blend only marginally change during the course of 60 minutes, suggesting that curing is largely prevented at these temperatures. The number of network points remains low, with only around 0.2 network points per 1000 carbons.

I then turned my attention to the electrical properties of p(E-*stat*-GMA$_{4.5}$):p(E-*stat*-AA$_3$) and ternary blends. For reference LDPE, a value of σ_{DC} ~ 2·10^{-16} S cm^{-1} at 70 °C is measured, while for p(E-*stat*-GMA$_8$):p(E-*stat*-AA$_7$):LDPE crosslinked blends (cured at 200 °C for 5 minutes) containing 20 to 50 wt% LDPE, σ_{DC} values of not more than 5·10^{-16} S cm^{-1} were measured at a temperature of 70 °C. I concluded that, despite the presence of polar comonomers, the conductivity of the here studied copolymer blends is hardly affected.

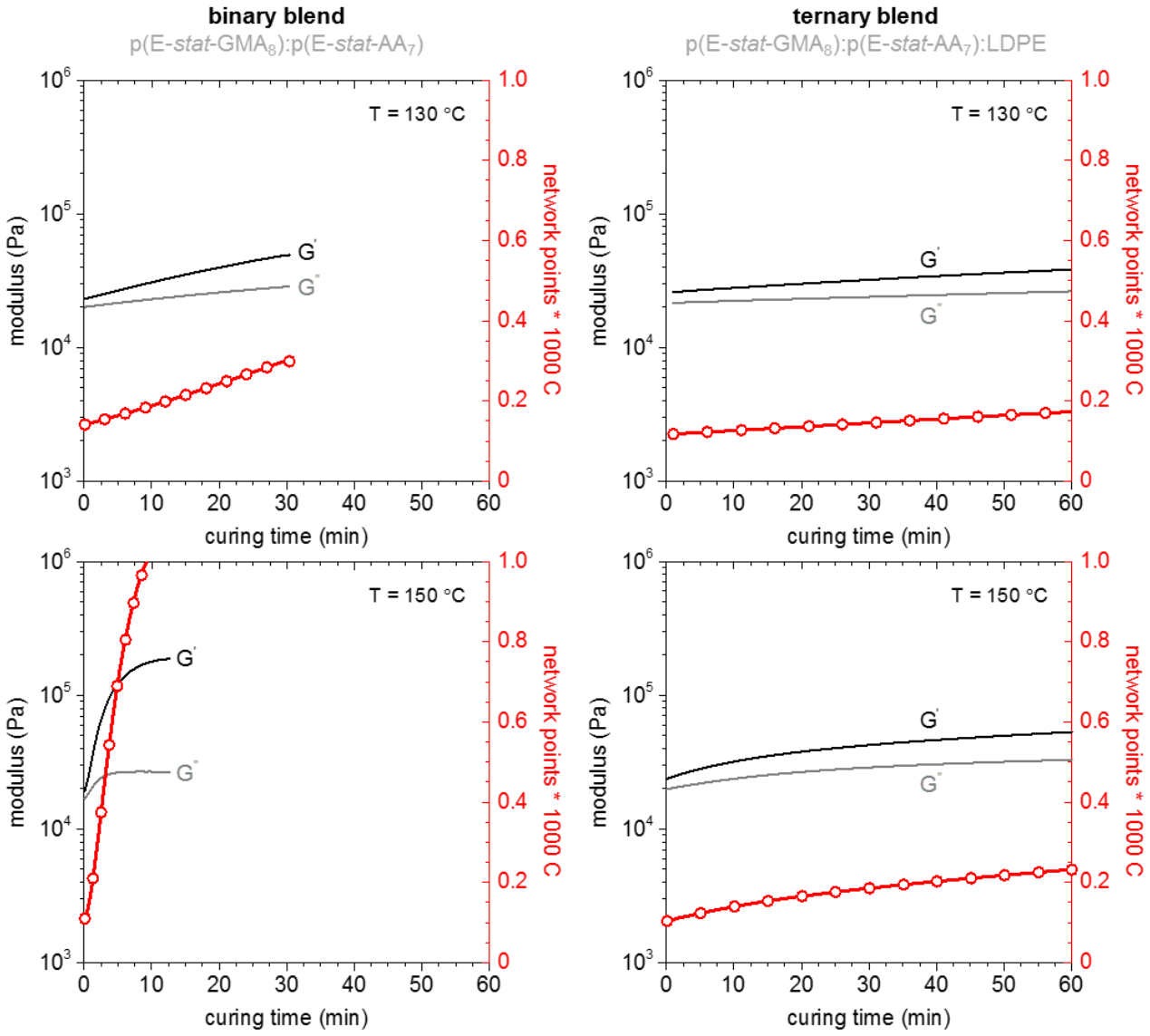

Figure 45: Storage and loss modulus, G' and G'', of the binary blend p(E-*stat*-GMA_8):p(E-*stat*-AA_7) (left) and the ternary blend p(E-*stat*-GMA_8):p(E-*stat*-AA_7):LDPE containing 50 wt% LDPE (right), measured by shear rheometry at 130 °C and 150 °C and a frequency of 1 Hz.

Outlook and conclusions

It is clear that HV cables will be a critical component of the future power grid that transports green energy to our homes, seamlessly integrating renewable sources of energy. The most advanced power cable technology uses XLPE insulation, which is produced by peroxide crosslinking of LDPE. This process gives rise to hazardous by-products that compromise the cleanliness of LDPE, and hence raise the electrical conductivity of the insulation material. Therefore, a byproduct free curing process, which maintains the processing advantages and high electrical resistivity of LDPE, is in high demand.

In this thesis, I have discussed different alternative concepts for the crosslinking of LDPE. I have established that epoxy click chemistry reactions can be effectively used to crosslink polyethylene-based copolymers, meeting industrial requirements for cable production but without the release of volatile by-products. The formulations discussed in this thesis offer a broad processing window, where compounding and shaping can be carried out without curing. At more elevated temperatures the carefully selected functional groups react without byproduct formation to form an infusible network. The concepts introduced in this thesis open up a number of questions that may serve as motivation for further studies. A more in-depth electrical characterization of the blends will help to understand the limits of the proposed alternative crosslinking concepts.

In order to gain more insight into the electrical properties of these materials, preliminary BDS experiments were carried out at low field strengths (~10-100 V mm^{-1}) (Figure 46). p(E-*stat*-GMA_8) blends crosslinked with low molecular weight curing agents (c.f. Paper I-II) show a σ_{DC} ~ 10^{-15} S cm^{-1}, compared to a σ_{DC} ~ 10^{-16} S cm^{-1} for standard XLPE. The higher conductivity is possibly linked to unreacted curing agents, which contribute to the ionic conductivity.

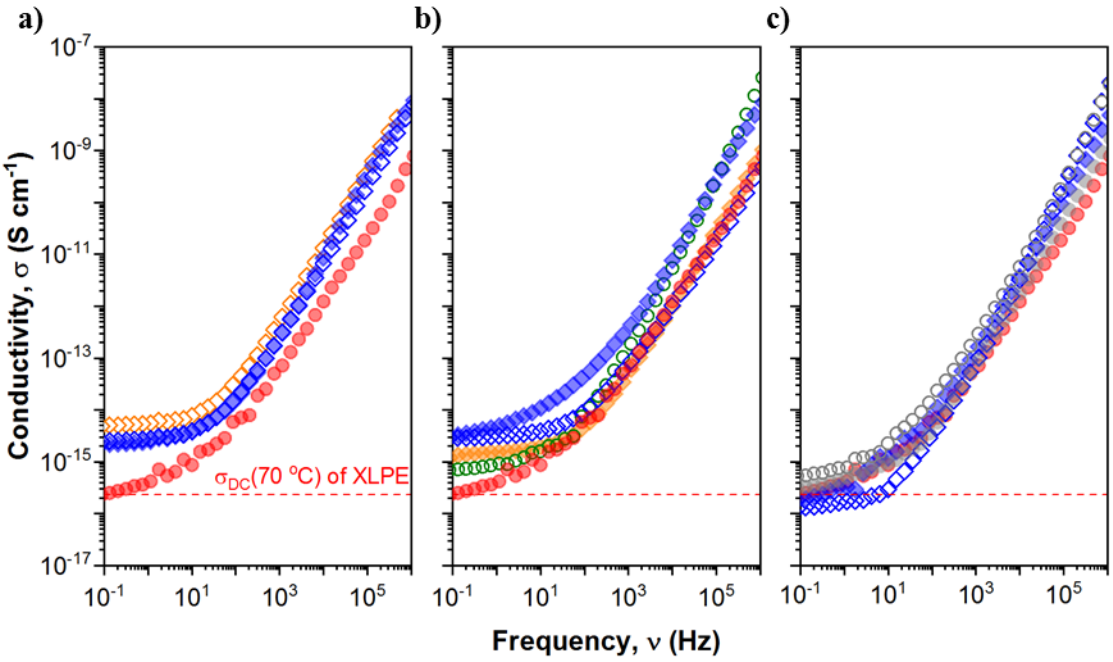

Figure 46: DC electrical conductivity measured at 70 °C for p(E-*stat*-GMA$_8$) cured for 5 minutes at 200 °C with different alternative crosslinking concepts, compared to XLPE (●): **a)** low molecular weight crosslinkers: DAO 1 % (◊), TMPTA 2 % (♦) and BPP 3 % (♦); **b)** Lewis acid catalysis: p(E-*stat*-GMA$_8$) (○), DAO 1 % (◊), TMPTA 2 % (♦) and BPP 3 % (♦) with 0.5 % Ti(2-EtHexO)$_4$; **c)** Copolymer blends: p(E-*stat*-AA$_8$):p(E-*stat*-GMA$_7$) with 0 % (◊), 30 % (●) and 50 % (○) neat LDPE, and p(E-*stat*-AA$_3$):p(E-*stat*-GMA$_{4.5}$).

Instead, crosslinked copolymer blends of two polyethylene copolymers (c.f. Paper III-IV) displayed a lower σ_{DC} of about 10^{-16} S cm^{-1} at 70 °C, which is at par with values measured for both ultra-clean LDPE and commercial XLPE. However, further characterization of the electrical properties of these materials is required. For example, it would be very interesting to perform DC measurements at high field strengths (e.g. 30 kV mm^{-1}), in order to gain more insight into the dielectric properties at high voltages.

Another important aspect that will require attention is the long-term stability. I performed preliminary aging studies on three selected blends, namely p(E-*stat*-GMA_8) cured with DAO, BPP:Ti(2-EtHexO)$_4$ and p(E-*stat*-AA_7). The storage modulus *G'* of specimens crosslinked for 20 minutes at 200 °C (stored in air at room temperature) was measured every 90 days, up to 540 days (Figure 47).

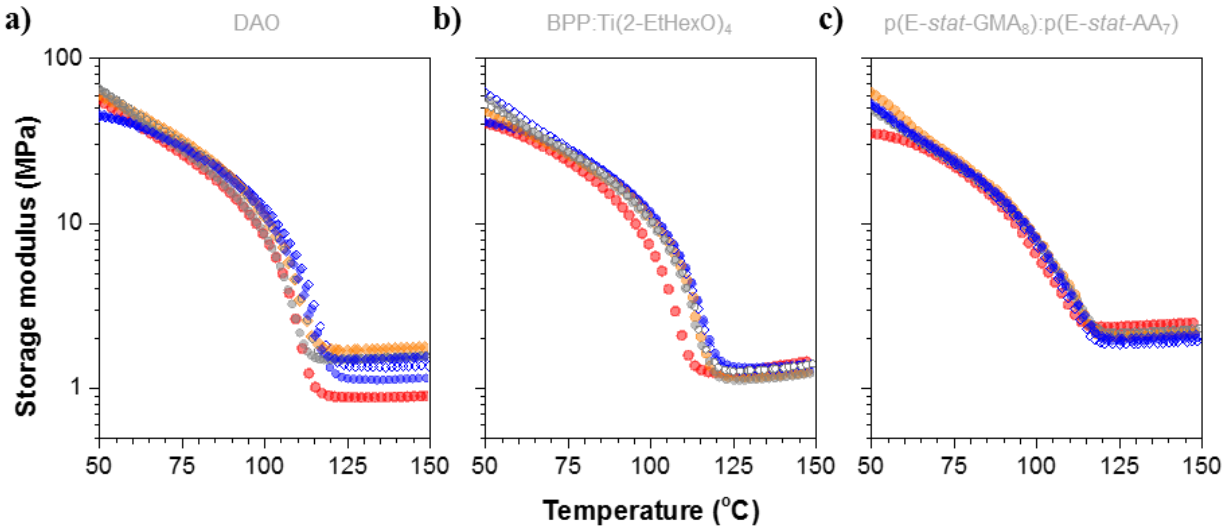

Figure 47: Storage modulus G' for p(E-*stat*-GMA_8) samples cured for 5 minutes at 200 °C with **a)** DAO **b)** BPP:Ti(2-EtHexO)$_4$ and **c)** p(E-*stat*-AA_7) and aged in air and room temperature for 1 (●), 90 (●), 180 (◊), 270 (♦), 360 (●), 450 (○) and 540 (♦) days.

Amine cured p(E-*stat*-GMA_8) shows a clear increase in rubber plateau values over time, which can be attributed to the fact that unreacted curing agent can slowly react with GMA functionalities even at room temperature, contributing to an increase in network density. BPP:Ti(2-EtHexO)$_4$ and p(E-*stat*-GMA_8):p(E-*stat*-AA_7) formulations however revealed to be very stable, with little to no change in the rubber plateau (Figure 48).

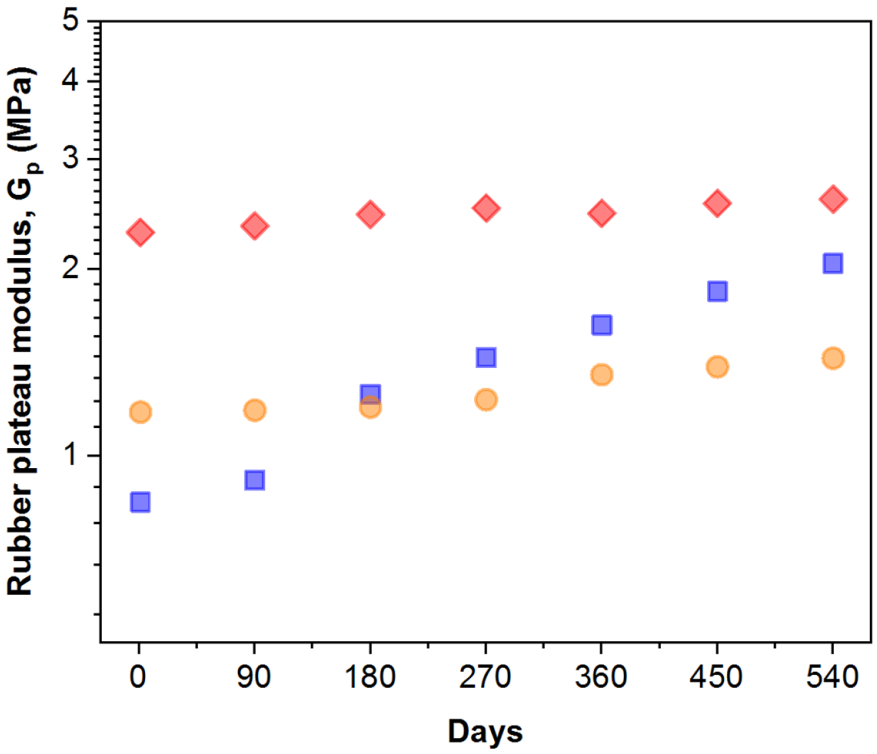

Figure 48: Rubber plateau modulus G_p for p(E-*stat*-GMA_8) samples cured for 5 minutes at 200 °C with DAO (■) BPP:$Ti(2\text{-EtHexO})_4$ and (●) p(E-*stat*-AA_7) (♦) and aged in air and room temperature for 1, 90, 180, 270, 360, 450 and 540 days.

Further studies, in particular accelerated aging at high temperature and aging of entire cables instead of single specimens (which means the insulation layer is protected from oxygen) will help to understand in more detail the stability of the insulation over a long period of time and consequently the lifespan of the cables, which ideally should last for decades.[103, 104] The copolymer blend route seems to be the most feasible process for replacing peroxide crosslinking, considering that such a system is additive-free, has similar mechanical and electrical properties as standard XLPE, is by-product free, and easy to implement.

Acknowledgements

I want to express my gratitude to Prof. Christian Müller, my main supervisor. It was a pleasure to work with you, I will never be able to thank you enough for believing in me and giving me the opportunity to be part of your research group at Chalmers. Thanks to your support and guidance I grew a lot, both from a professional and personal point of view. You have been the best supervisor I could ask for, thank you for sharing your passion for science with me.

I also want to thank my co-supervisor Oscar Prieto. I have really enjoyed all our discussions and I appreciated your support during my studies. Thank you for your invaluable scientific inputs and for starting the exciting work on epoxy crosslinking that led to this project.

Thomas Gkourmpis, it was an absolute pleasure to have the chance to share so many moments and discussions about science and life with you. I enjoyed working together, thank you for all your advice and for always giving me your honest opinion.

I want to thank Borealis AB in Stenungsund and in particular Martin Anker, Thomas Hjertberg, Per-Ola Hagstrand and Diana Gómez-Heincke. Thanks for the guidance, the support, the expertise and the appreciation you have provided me during these years.

Thanks to all my friends at the 8th floor, especially to Lotta Pettersson and my colleagues in the Müller research group. Jonna, David, Amaia, Yingwei, Sepideh, Ida, Liyang, Renee, Anja, Anna, I have learned something from each of you, and you will always be with me in my heart.

Jason Ryan, you were the first one to greet me at the airport once I landed in Sweden at the beginning of this journey, and the last one to say goodbye once I moved to Norway at the end of it. Thank you, my friend, for all the moments we shared.

A big thank you to Anna Peterson, it was a pleasure to work with you on our paper! I wish you the best for your studies.

Thank you Alicja for all the coffees we shared and all the discussions we had, and for all the sugar free drinks you left on my desk on your way back from lunch. They will not be forgotten!
Big thanks also go to my friend and former colleague Mattias Andersson, for always being there for me whenever I needed help at the beginning of my PhD.

I also want to thank my friends outside Chalmers, with extra love to Luis Aguilera. Gracias, mi hermano, por todos los entrenamientos, las discusiones, los viajes, las fiestas y la diversión que tuvimos juntos. ¡Nos lo pasamos muy bien! Hiciste mi vida en Suecia mucho más colorida.

Un grazie speciale va ai miei genitori, Nicoletta e Maurizio. Ogni traguardo che raggiungo è anche un traguardo vostro: non sarei qui oggi senza il vostro amore, il vostro supporto ed i vostri sacrifici. Grazie per aver sempre creduto in me, per avermi insegnato il valore dello studio, del lavoro e della dedizione. Sono orgoglioso di avervi come genitori, non avrei potuto desiderare un amore più grande del vostro.
Grazie mille anche a mio fratello Alessandro. Sono orgoglioso dell`uomo e del professionista che sei diventato. Ti auguro il meglio, sia nella vita che nel lavoro, e di raggiungere tutti gli obiettivi che ti prefiggerai.

Marita, simply writing your name puts a smile on my face. My life has been amazing since the day I met you, and I feel so privileged to share it with you. Thanks for all the love you have for me, it`s my greatest strength. As long as I can see your smile when I wake up in the morning, and I can kiss you before going to bed at night, I`m the richest man in the world. Jeg elsker deg.

References

1. E. Peschke and R. von Olshausen, *Cable System for High and Extra-High Voltage* Pirelli, 1999.
2. E. Kuffel, W. S. Zaengl and J. Kuffel, *High Voltage Engineering: Fundamentals*, Elsevier Ltd., Jordan Hill, Oxford, 2000.
3. G. Mazzanti and M. Marzinotto, *Extruded Cables for High-Voltage Direct-Current Transmission*, Wiley, Hoboken, 2013.
4. K.-G. Fricke, R. Paschen and R.-D. Steckel, *Overhead and Underground HV Lines - Comparison and new Aspects*, CIGRE, Paris, 1996.
5. Y. Murata, M. Sakamaki, K. Abe, Y. Inoue, S. Mashio, S. Kashiyama, O. Matsunaga, T. Igi, M. Watanabe, S. Asai and S. Katakai, SEI Technical Review, 2013.
6. G. Asplund, L. Carlsson and O. Tollerz, *50 years HVDC*, ABB Review, 2003.
7. *European commission: Energy Roadmap 2050*, 2012, ISBN 978-92-79-21798-2.
8. M. G. Andersson, J. Hynynen, M. R. Andersson, P. O. Hagstrand, T. Gkourmpis and C. Müller, *J. Polym. Sci. Pol. Phys.*, 2017, **55**, 146-156.
9. V. Englund, J. Andersson, J.-O. Boström, V. Eriksson, P.-O. Hagstrand, J. Jungqvist, W. Loyens, U. H. Nilsson and A. Smedberg, *Characteristics of Candidate Material Systems for next Generation Extruded HVDC Cables*, CIGRE, Paris, 2014.
10. M. G. Andersson, M. Jarvid, A. Johansson, S. Gubanski, M. R. S. Foreman, C. Müller and M. R. Andersson, *Eur. Polym. J.*, 2015, **64**, 101-107.
11. M. G. Andersson, J. Hynynen, M. R. Andersson, V. Englund, P. O. Hagstrand, T. Gkourmpis and C. Müller, *ACS Macro. Lett.*, 2017, **6**, 78-82.
12. M. Jarvid, A. Johansson, R. Kroon, J. M. Bjuggren, H. Wutzel, V. Englund, S. Gubanski, M. R. Andersson and C. Müller, *Adv. Mater.*, 2015, **27**, 897-902.
13. E. Malmström, H. Hillborg, A. Carlmark, C. Sanchez and M. Wahlander, *Reduced and Surface-Modified Graphene Oxide with Nonlinear Resistivity*, 254th National Meeting and Exposition of the American-Chemical-Society (ACS) on Chemistry's Impact on the Global Economy, Washington DC, Aug 20, 2017.
14. M. Wahlander, F. Nilsson, R. L. Andersson, A. Carlmark, H. Hillborg and E. Malmström, *Macromol. Rapid. Comm.*, 2017, **38**.
15. M. Wahlander, F. Nilsson, R. L. Andersson, C. C. Sanchez, N. Taylor, A. Carlmark, H. Hillborg and E. Malmström, *J. Mater. Chem. A*, 2017, **5**, 14241-14258.
16. M. Mauri, A. Peterson, A. Senol, K. Elamin, A. Gitsas, T. Hjertberg, A. Matic, T. Gkourmpis, O. Prieto and C. Müller, *J. Mater. Chem. C*, 2018, **6**, 11292-11302.

17. M. Mauri, N. Tran, O. Prieto, T. Hjertberg and C. Müller, *Polymer*, 2017, **111**, 27-35.
18. M. Mauri, L. Svenninsson, T. Hjertberg, L. Nordstierna, O. Prieto and C. Müller, *Polym. Chem.*, 2018, **9**, 1710-1718.
19. A. Gustafsson, M. Saltzer, A. Farkas, H. Ghorbani, T. Quist and M. Jeroense, *The new 525 kV extruded HVDC cable system*, ABB press release, 2014.
20. P. Bergelin, M. Jeroense, T. Quist and H. Rapp, *640 kV extruded HVDC cable system: World´s most powerful extruded cable system*, NKT press release, 2017.
21. G. C. Montanari, P. H. F. Morshuis, M. Zhou, G. C. Stevens, A. S. Vaughan, Z. Han and D. Li, *IET High Voltage*, 2017, **3**, 90-95.
22. Elforsk, *Enmegavoltsutmaningen*, 2014.
23. A. M. Pourrahimi, R. T. Olsson and M. S. Hedenqvist, *Adv. Mater.*, 2018, **30**, 1703624.
24. H. Ghorbani, M. Jeroense, C. O. Olsson and M. Saltzer, *IEEE Trans. Power Del.*, 2014, **29**, 414-421.
25. M. Jeroense, *IEEJ Trans. Electr. Electron. Eng.*, 2010, **5**, 400-404.
26. L. A. Dissado and J. C. Fothergill, *Electrical Degradation and Breakdown in Polymers*, Peter Peregrinus Ltd., 1992.
27. U. H. Nilsson, *The use of model cables for the evlauation of the electrical performance of polymeric power cable materials*, NORD-IS 05, Trondheim, 2005.
28. B. Holmgren and S. Hvidsten, *Status of Condition Assessment of water treed 12 and 24 kV XLPE cables in Norway and Sweden*, NORD-IS 05, Trondheim, 2005.
29. H. Sarma, E. Cometa and J. Densley, *IEEE Electr. Insul. Mag.*, 2002, **18**, 15-26.
30. H. Aoyama, K. Matsui, Y. Tanaka, T. Takada and T. Maeno, *Observation and numerical analysis of space charge behaviour in low-density polyethylene formed by ultra-high DC stress*, Annual Report Conference on Electrical Insulation and Dielectric Phenomena (CEIDP), 2005, 445-448.
31. Z. Yewen, J. Lewiner, C. Alquie and N. Hampton, *IEEE Trans. Dielectr. Electr. Insul.*, 1996, **3**, 778-783.
32. M. Unge, T. Christen and C. Tornkvist, *Electronic structure of polyethylene - Crystalline and amorphous phases of pure polyethylene and their interfaces*, 2012 Annual Report Conference on Electrical Insulation and Dielectric Phenomena (CEIDP), 2012, 525-530.
33. M. P. De Haas, A. Hummel and J. M. Warman, *Synth. Met.*, 1991, **41**, 1255-1258.
34. L. H. Chen, T. D. Huan and R. Ramprasad, *Sci. Rep.*, **7**, 2017.
35. P. S. Chum and K. W. Swogger, *Prog. Polym. Sci.*, 2008, **33**, 797-819.
36. D. B. Malpass, *Introduction to Industrial Polyethylene: Properties, Catalysts Processes*, Wiley, 2010.

37. A. Vaughan, D. S. Davis and J. R. Hagadorn, *Polymer Science: A Comprehensive Reference*, 2012, **3**, 657-672.
38. I. Chodak, *Prog. Polym. Sci.*, 1995, **20**, 1165-1199.
39. M. Lazar, R. Rado and J. Rychly, *Adv. Polym. Sci.*, 1990, **95**, 149-197.
40. R. Patterson, A. Kandelbauer, U. Müller and H. Lammer, *Crosslinked thermoplastics*, Elsevier, 2014.
41. G. B. Shah, M. Fuzail and J. Anwar, *J. Appl. Polym. Sci.*, 2004, **92**, 3796-3803.
42. A. Smedberg, T. Hjertberg and B. Gustafsson, *Polymer*, 1997, **38**, 4127-4138.
43. T. Knobel and P. R. Minbiole, *US Patent 5,916,929*, 1997.
44. M. Severengiz, T. Sprenger and G. Seliger, *Proc. CIRP*, 2016, **40**, 18-23.
45. D. A. Ivanov, *Polymer Science: A Comprehensive Reference*, 2012, **1**, 227-258.
46. A. D. Jenkins, P. Kratochvil, R. F. T. Stepto and U. W. Suter, *Pure Appl. Chem.*, 1996, **68**, 2287-2311.
47. M. Pire, S. Norvez, I. Iliopoulos, B. Le Rossignol and L. Leibler, *Compos. Interfaces*, 2014, **21**, 45-50.
48. C. V. Chaudhari, Y. K. Bhardwaj, N. D. Patil, K. A. Dubey, V. Kumar and S. Sabharwal, *Radiat. Phys. Chem.*, 2005, **72**, 613-618.
49. A. Chapman and T. Johnson, The role of zinc in the vulcanisation of styrene-butadiene rubbers, KGK - *Kaut. Gummi Kunst.*, 2005, **58**, 358-361.
50. C. Beveridge and A. Sabiston, *Mater. Des.*, 1987, 263-268.
51. W. Zhou and S. Zhu, *Macromolecules*, 1998, **31**, 4335-4341.
52. M. Palmlof, T. Hjertberg and B. A. Sultan, *J. Appl. Polym. Sci.*, 1991, **42**, 1193-1203.
53. L. Minkova, M. Nikolova and E. Nedkov, *J. Macromol. Sci. Phys.*, 1988, **B27**, 99-118.
54. F. M. Precopio and A. R. Gilbert, *US Patent 3,079,370*, 1955.
55. F. Precopio, *IEEE Electr. Insul. Mag.*, 1999, **15**, 23-25.
56. T. Andrews, R. N. Hampton, A. Smedberg, D. Wald, V. Waschk and W. Weissenberg, *IEEE Electr. Insul. Mag.*, 2006, **22**, 5-16.
57. J. Sahyoun, A. Crepet, F. Gouanve, L. Keromnes and E. Espuche, *J. Appl. Polym. Sci.*, 2017, **134**.
58. G. Tillet, B. Boutevin and B. Ameduri, *Prog. Polym. Sci.*, 2011, **36**, 191-217.
59. B. I. Chaudhary, S. S. Sengupta, J. M. Cogen and M. Curio, *Polym. Eng. Sci.*, 2011, **51**, 237-246.
60. S. Dabdin, M. Frounchi, M. Haji Saeid and F. Gangi, *J. Appl. Polym. Sci.*, 2002, **86**, 1959-1969.
61. K. Makuuchi and S. Cheng, *Radiation processing of polymer materials and its industrial applications*, John Wiley & Sons, Hoboken, 2012.
62. R. Basheer and M. Dole, *J. Polym. Sci. B Polym. Phys.*, 1983, **21**, 949-956.

63. M. A. Rodriguez-Perez, *Crosslinked Polyolefin Foams: Production, Structure, Properties, and Applications*. In: *Crosslinking in Materials Science. Advances in Polymer Science*, Springer, Berlin, Heidelberg, 2005, **184**, 97-126.
64. E. C. L. Cardoso, S. R. Scagliusi, D. F. Parra and A. B. Lugao, *Radiat. Phys. Chem.*, 2013, **84**, 170-175.
65. M. Dole, *ACS Symp. Series*, 1983, **229**, 17-24.
66. H. C. Kolb, M. G. Finn and K. B. Sharpless, *Angew. Chem. Int. Ed.*, 2001, **40**, 2004-2021.
67. C. E. Hoyle, A. B. Lowe and C. N. Bowman, *Chem. Soc. Rev.*, 2010, **39**, 1355-1387.
68. B. Helms, J. L. Mynar, C. J. Hawker and J. M. J. Frechet, *J. Am. Chem. Soc.*, 2004, **126**, 15020-15021.
69. N. W. Polaske, D. V. McGrath and J. R. McElhanon, *Macromolecules*, 2011, **44**, 3203-3210.
70. R. D. B. Garcia, L. Keromnes, Y. Goutille, P. Cassagnau, F. Fenouillot and P. Chaumont, *Eur. Polym. J.*, 2014, **61**, 186-196.
71. H. Q. Pham and M. J. Marks, *Epoxy Resins*, Wiley-VCH, Weinheim, Germany, 2006.
72. Y. Yu, M. Z. Rong and M. Q. Zhang, *Polymers & Polymer Composites*, 2012, **20**, 673-681.
73. Q. Wei, D. Chionna, E. Galoppini and M. Pracella, *Macromol. Chem. Phys.*, 2003, **204**, 1123-1133.
74. L. Xu, J. H. Fu and J. R. Schlup, *J. Am. Chem. Soc.*, 1994, **116**, 2821-2826.
75. K. C. Cole, J. J. Hechler and D. Noel, *Macromolecules*, 1991, **24**, 3098-3110.
76. X. Colin, C. Marais and J. Verdu, *Polym. Test.*, 2001, **20**, 795-803.
77. P. Campaner, D. D'Amico, L. Longo, C. Stifani and A. Tarzia, *J. Appl. Polym. Sci.*, 2009, **114**, 3585-3591.
78. A. Gardziella, L. Pilato and A. Knop, *Phenolic resins : chemistry, applications, standardization, safety, and ecology*, Springer, Berlin ; New York, 2nd completely rev. edn., 2000.
79. J. A. Carioscia, J. W. Stansbury and C. N. Bowman, *Polymer*, 2007, **48**, 1526-1532.
80. S. Binder, I. Gadwal, A. Bielmann and A. Khan, *J. Polym. Sci. Pol. Chem.*, 2014, **52**, 2040-2046.
81. A. Kumar, R. R. Ujjwal, A. Mittal, A. Bansal and U. Ojha, *ACS Appl. Mater. Interfaces*, 2014, **6**, 1855-1865.
82. A. M. Tomuta, X. Ramis, F. Ferrando and A. Serra, *Prog. Org. Coatings*, 2014, **74**, 59-66.
83. R. Alex, P. P. De and S. K. De, *J. Polym. Sci. Polym. Lett.*, 1989, **27**, 361-367.
84. J.-P. Pascault and J. J. R. Williams, *Epoxy Polymers, New Materials and Innovations*, Wiley-VCH, Weinheim, Germany, 2010.
85. K. Dušek and R. Dave, *Epoxy resins and composites IV*, Springer-Verlag, Berlin ; New York, 1986.
86. R. Auvergne, S. Caillol, G. David, B. Boutevin and J. P. Pascault, *Chem. Rev.*, 2014, **114**, 1082-1115.

87. J. Leukel, W. Burchard, R. P. Kruger, H. Much and G. Schulz, *Macromol. Rapid Commun.*, 1996, **17**, 359-366.
88. N. Torres, J. J. Robin and B. Boutevin, *J. Appl. Polym. Sci.*, 2001, **81**, 581-590.
89. N. Torres, J. J. Robin and B. Boutevin, *J. Appl. Polym. Sci.*, 2001, **81**, 2377-2386.
90. Q. Wei, D. Chionna and M. Pracella, *Macromol. Chem. Phys.*, 2005, **206**, 777-786.
91. Y. W. Xu, J. Loi, P. Delgado, V. Topolkaraev, R. J. McEneany, C. W. Macosko and M. A. Hillmyer, *Ind. Eng. Chem. Res.*, 2015, **54**, 6108-6114.
92. J. E. White, H. C. Silvis, M. S. Winkler, T. W. Glass and D. E. Kirkpatrick, *Adv. Mater.*, 2000, **12**, 1791-1800.
93. M. N. Mang, J. E. White, S. L. Kram, D. L. Rick, R. E. Bailey, and P. E. Swanson, *Polym. Mater. Sci. Eng.*, 1997, **76**, 412-413.
94. M. N. Mang, J. E. White, A. P. Haag, S. L. Kram and C. N. Brown, *Polym. Prepr., (ACS, Div. Polym. Chem.)*, 1995, **210**, 186
95. S. A. Kumar, T. Balakrishnan, A. Alagar and Z. Denchev, *Prog. Org. Coat.*, 2006, **55**, 207-217.
96. D. J. Brennan, J. E. White, A. P. Haag, S. L. Kram, M. N. Mang, S. Pikulin and C. N. Brown, *Macromolecules*, 1996, **29**, 3707-3716.
97. International Electrotechnical Commission, *IEC 60811-507:2012 Electric and optical fibre cables - Test methods for non-metallic materials*, 2012.
98. E. P. Otocka and T. K. Kwei, *Macromolecules*, 1968, **1**, 244-249.
99. A. Taubert and K. I. Winey, *Macromolecules*, 2002, **35**, 7419-7426.
100. K. Wakabayashi and R. A. Register, *Macromolecules*, 2006, **39**, 1079-1086.
101. J. P. Flory, *Networks, Encyclopedia of Polymer Science and Engineering*, Wiley, 1987.
102. C. Y. Liu, J. S. He, E. van Ruymbeke, R. Keunings and C. Bailly, *Polymer*, 2006, **47**, 4461-4479.
103. L. Wenyuan, E. Vaahedi and P. Choudhury, *IEEE Power Energy Mag.*, 2006, **4**, 52-58.
104. N. Hampton, R. Hartlein, H. Lennartsson, H. Orton and R. Ramachandran, *Long-life XLPE-insulated Power Cables*, 7th International Conference on Power Insulated Cables (JICABLE), Versailles, 2007.